Fabrication of a Dye Sensitized Solar Cell using blackberry dye: Effect of $TiCl_4$ as blocking layer

Submitted by:

Masrura Qazi

Examination Roll: 523

Reg. No: HA 214; Session: 2014-15

M.S. THESIS

Institute of Energy

University of Dhaka

September, 2016

Fabrication of a Dye Sensitized Solar Cell using blackberry dye: Effect of $TiCl_4$ as blocking layer

A Dissertation Submitted for the Partial Fulfillment for the Degree of Master of Science in Renewable Energy

Joint Supervision of:

Prof. Dr. Saiful Hoque

Director and Professor

Institute of Energy, University of Dhaka

Professor Dr. Mubarak Ahmad Khan

Chief Scientific Officer (CSO) & Director General

Bangladesh Atomic Energy Research Establishment (AERE)

Dr. Mosharraf Hossain Bhiuyan

Principal Scientific Officer, Institute of Nuclear Science and Technology (INST)

Bangladesh Atomic Energy Research Establishment (AERE)

Keywords: Nanoparticle, Organic Dye, Porosity, Blocking Layer, Electrolyte

Certificate of Authentication

This is to certify that the Thesis Report entitled "Fabrication of a dye sensitized solar cell using blackberry dye: Effect of $TiCl_4$ as blocking layer" submitted by Masrura Qazi of Masters (Class roll: 39, Exam roll: 523, Session 2014-2015) was prepared under my instruction and direct supervision.

Prof. Dr. Saiful Hoque
Director and Professor
Institute of Energy
University of Dhaka

Declaration

I, Masrura Qazi, a student of Masters in Science in Renewable Energy Technology at the Institute of Energy, University of Dhaka hereby declare that this thesis and the research work presented in this thesis titled "Fabrication of a dye sensitized solar cell using blackberry dye: Effect of $TiCl_4$ as blocking layer" is my own and has been performed by myself. The data obtained and the results generated are a result of my own work at the Dye-Sensitized Solar Cell Laboratory at Institute of Radiation and Polymer Technology (IRPT), Bangladesh Atomic Energy Research Establishment (AERE).

Masrura Qazi
Exam roll: 523, Class roll: 39
Session: 2014-2015
Institute of Energy, University of Dhaka.

Acknowledgement

All praise goes to Almighty Allah for His blessings and mercy upon me for completion of this thesis. Acknowledgements are gratefully made to my respected supervisors, Professor Dr. Saiful Hoque, along with Professor Dr. Mubarak Ahmad Khan, Chief Scientific Officer (CSO) & Director General, Bangladesh Atomic Energy Research Establishment (AERE) and Dr. Mosharraf Hossain Bhiuyan, Principal Scientific Officer, Institute of Nuclear Science and Technology (INST), Bangladesh Atomic Energy Research Establishment (AERE) for their whole hearted guidance, patience, constructive advice and instructions, and also for making themselves available whenever it was needed.

I am most indebted to Professor Dr. Mubarak Ahmad Khan, Chief Scientific Officer (CSO) & Director General, Bangladesh Atomic Energy Research Establishment (AERE) for providing me with the opportunity to carry out a research at the prestigious organization of Institute of Radiation and Polymer Technology (IRPT), Bangladesh Atomic Energy Research Establishment (AERE) at the Dye-Sensitized Solar Cell Laboratory. Other people from whom I benefited in this research including, within and outside of the group: Dye Sensitized Solar Cell Laboratory, Institute of Radiation and Polymer Technology (IRPT), Bangladesh Atomic Energy Research Establishment (AERE). I have enjoyed doing research and discussing experimental details with them. Without their help, many things could have been much more difficult to achieve. I am also grateful to Md. Saifur Rahman, Scientific Officer, Institute of Radiation and Polymer Technology (IRPT), Bangladesh Atomic Energy Research Establishment (AERE) and Jahid Mahbub, Bangladesh Atomic Energy Research Establishment for their undying guidance and support throughout my thesis. Gratitude and thanks are due to Shahriar Bashar, Scientific Officer, Bangladesh Council of Scientific and Industrial Research (BCSIR)for his help with scanning electron microscopy (SEM). His patience in helping me operate the equipment is greatly appreciated.

Best regards and special thanks to all my classmates and friends and reasearch fellows, particularly Touhidul Islam, Tania Akhter Ruhanne and Toriqul Islam Bhuiyan at AERE for their support and cooperation. My heartfelt gratitude towards my siblings who have provided me with lots of encouragement and support in the completion of this work and would like to thank my parents for their prayers, continuous moral support and belief in me. Thanks to IDCOL for providing financial support under AERE-IDCOL solar cell project on “Fabrication and Characterization of Dye Sensitized Solar Cell (DSSC) using natural dye and its impact in Bangladesh” for completion of this research work. In addition, thanks to Ministry of Science & Technology, GOB, for providing partial support under special allocation for this research work.

Masrura Qazi (Exam Roll: 523; Class Roll: 39)
Session: 2014-15
Institute of Energy, University of Dhaka

Table of Contents

LIST OF FIGURES

LIST OF TABLES

ABSTRACT

Energy crisis is one of the most pressing issues of the world. Increasing industries and luxuries have made energy limited compared to the demand for it and the reserve in fossil fuel. An alternative to this crisis is the inorganic and organic solar cell. Organic solar cell having a cost effective prospective is highly demanding.

During this research work, a prototype of dye-sensitized solar cell was developed using organic dye from blackberry and TiO_2 nanocrystals paste was used as semiconductor. All work was done in the dye-sensitized solar cell lab of Bangladesh Atomic Energy Commission in joint collaboration with University of Dhaka. The TiO2 and the ITO glasses were imported while the dye was obtained locally. The developed cell was tested for measurement of efficiency in a lab-constructed simulator where the irradiation was provided with a halogen lamp of 20 Watt/220 Volt with intensity of around 900 W/m2 at a distance of 30cm. The characterization of the cell gives I-V characteristics with open circuit voltage of 440 mV, short circuit current of 600μA, fill factor of 45.67 %, and energy efficiency of 0.03 % for raw dye. An improved cell current and cell-voltage was observed when the dye was extracted by soaking in ethanol, for which the characterization of the cell gives I-V characteristics with open circuit voltage of 497mV, short circuit current of 943μA, fill factor of 40.61 %, and energy efficiency of 0.05 %. However it was found with more improved cell efficiency when post treatment was performed on the titanium dioxide layer; the improved cell efficiency being 0.0869%. The solar cell shows degradation in performance with open circuit voltage and short circuit current degrading gradually.

Chapter 1

1.1 INTRODUCTION

Energy is a daily requirement for us to survive. Starting from a morning breakfast to obtaining fresh water till getting back to bed. The current total world consumption for energy is continuously expanding. It has expanded from 549 quadrillion British thermal units (Btu) in 2012 to 629 quadrillion Btu in 2020 and is expected to reach 815 quadrillion Btu in 2040, which a 48% increase from 2012 to 2040[1]. Fossil fuels including coal, oil and gas alone are insufficient to meet the demand. Renewable energy sources has been aide to this crisis. Photovoltaic cells, for generation of electricity, was initially developed in the early 20th century while commercially viable model made its appearance using silicon technology in the mid-20th century. The energy crisis of the 1970s brought about an increased interest in the technology to help try and mitigate energy crisis. Researchers dedicated their attention to bring in changes with the help of technology to the silicone industries of photovoltaic cells. With the microchip industry also rising demand for silicon increased making photovoltaic cells expensive, in achieving purity of silicon for production, compared to the efficiency obtained.

A second option to obtain electricity directly from solar energy is the organic solar cells which imitates the photosynthetic process for energy conversion. The ease of procuring while a low need for purity of the raw materials makes these cells affordable and largely demanding. The new class of organic solar cell developed by Michael Gratzel and Brian O'Regean in 1991 using titanium dioxide as comparatively inexpensive semiconductors and organic or synthetic dyes as synthesizers was another breakthrough. Although the commercial viability is still in question owing to the still low efficiency and a few other factors.

The beginning of the organic cells have been slow however there has been a significant increase in efficiency and durability in the lab. On the other hand silicon based cells has had an increase in cost because of the worldwide increase in the consumption of hyper-pure silicon. Soon organic solar cells can be expected to replace the silicon based solar cell industry owing to the cost issue.

Research to evaluate relationships of the various components to ascertain how they interact with one another would be beneficial to understanding how to improve overall efficiency of dye sensitized cells. This will increase understanding of how all of the components work together, and which contribute the most to overall efficiency.

This study combines the search for a different approach for making titanium dioxide paste, an efficient dye extraction process and the effect of blocking layer using a titanium tetra-chloride solution to increase the cell current to improve efficiency. Also to observe the combined effect of these factors.

1.2 THESIS OUTLINE

The remainder of this thesis is organized as follows:

Chapter 2: Describes the available energy resources world wide and in Bangladesh along with the limitations of the available energy forms. It also includes the history of development of solar cell and DSSC

Chapter 3: Includes a literature review designed to provide a summary of the base of knowledge already available involving the issues of interest. It presents the research works on different components of DSSC by various researches.

Chapter 4: Includesthe techniques involved in fabrication and characterizaton of DSSC with the details of experimental procedure that has been followed.

Chapter 5: Presents the results which is explained for each data obtained during the experiment.

Chapter 6: Provides summary of the findings of this research work and suggests ideas and directions for future research.

Chapter 2

2.1 ENERGY SOURCES AND THEIR LIMITATIONS

Energy needs world wide has been a big issue. The limited energy resources available has made the need for conduction of statistical analyses. Although there has been a number of ways to conduct analyses, the use of analysis of variance is a much more accepted method. The overall variability in the data is easily comparable, in this method, with the variability, it is possible to determine which the factors or combinations of factors are statistically significant.

2.1.1 World Energy Statistics

Energy by definition is the ability for a body to perform work. It is a property of objects which can be transferred to other objects or converted into different forms. Modern life is almost at a stand still point without energy. It is very closely related everything we do. Without energy nothing gets done. All sectors of our modern life starting from transports to electricity production, food production toheating, lightening, manufacturing, cooling and refining are all depended on energy most of which is provided from fuel energy. Lheuxuries and industries require humongous amount of energy making the rich nations most energy consuming nations. Hoever, energy is in a way the key element for everything modern in this developing society.

Sources of energy

Energy can be classified into two categories:

I. Non Renewable Energy
II. Renewable Energy

i. Non-Renewable Energy Sources: an energy resource that is not replaced or is replaced only very slowly by natural processes.
   - Conventional: This category includes:
     - Petroleum

- Natural Gas
- Coal
- Nuclear

- Unconventional:
  - Oil Shale
  - Natural gas hydrates in marine sediment

ii. Renewable Energy Sources: Renewable energy sources are the natural resources such as sunlight, wind, rain, tides, and geothermal heat can be and are used to generate renewable energy. These are known as renewable since they are naturally replenished. About 16% of global final energy consumption comes from renewable, with 10% coming from traditional biomass, which is mainly used for heating, and 3.4% from hydroelectricity. New renewables (small hydro, modern biomass, wind, solar, geothermal, and biofuels) accounted for another 3% and are growing very rapidly. The share of renewables in electricity generation is around 19%, with 16% of global electricity coming from hydroelectricity and 3% from new renewables. Coupled renewable sources are another option in generation of energy. The cogeneration and trigeneration are bringing in changes along with positive aspects by helping several enrgy functions being satisfied together. Some of the common renewable energy resources include:

- Solar energy
- Wind
- Hydropower
- Biomass
- Ocean energy
- Geothermal
- Waste to Energy

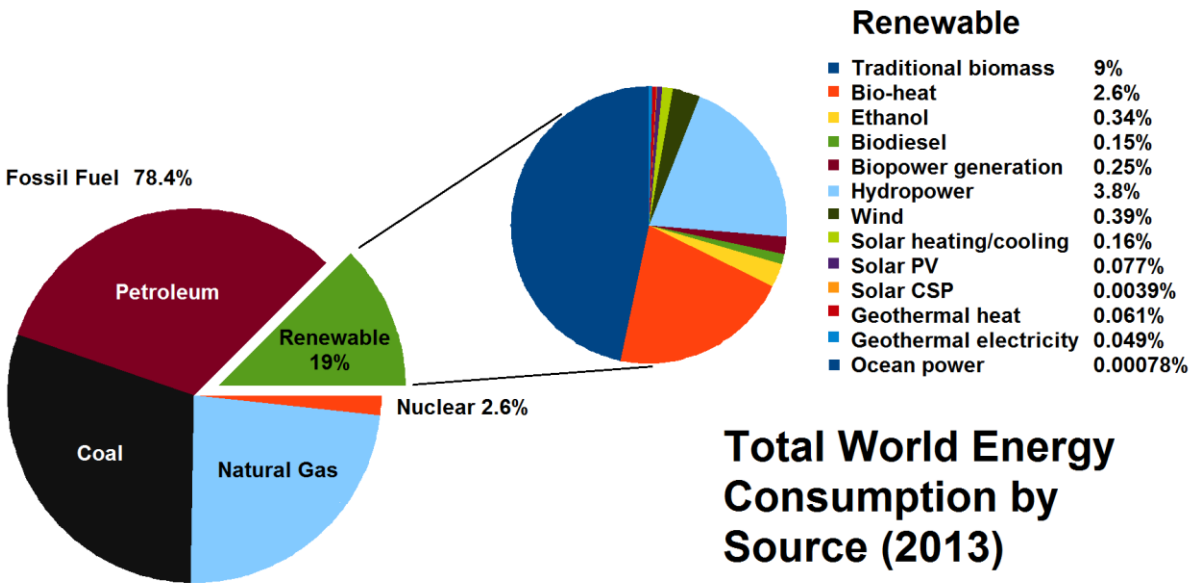

Figure 1 Total World Consumption by Source (2013) Source: wikipedia

2.1.2 World Fossil Fuel Reserve and Consumption:

Crude oil, coal and gas are the main resources for world energy supply.

2.1.2.1 Crude oil

Crude oil is a naturally occurring liquid composed mostly of hydrogen and carbon. It is usually found underground. Present world demand is 91.4 million barrels a day, which each year is nearing 3% per year of known reserves. Reserves are put at 2686 billion barrels, plus 850 billion barrels in oil shale (also referred to as unconventional oil). Many expect peak production by 2015 after which it would become very expensive: but future needs vary between 65 and 120 million barrels by 2030.

Optimistic hopes are that 1 trillion barrels remain to be found. There is expected to be a smooth in oil production between 2015 and 2100. After this there will be a steady decline and price rise. Extraction from oil shale/tar oil sands is difficult and takes large quantities of water and heat in the process of extraction so increasing the CO2 emissions.

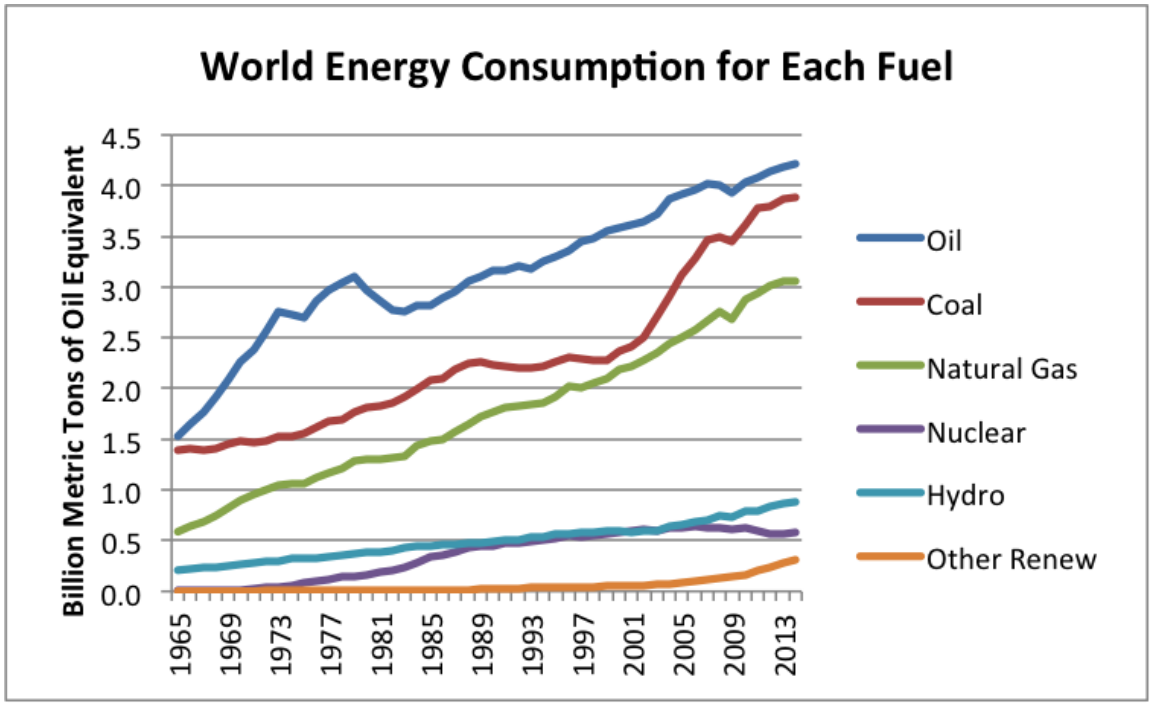

Figure 2 World Energy Consumption for Each Fuel Source: wikipedia

2.1.2.2 Natural Gas

Known gas reserves (5150 trillion cu feet) could probably last for 65 years at the current rate of use (220 billion cu feet a day) but it is thought that there could be 8500 trillion cu feet including reserves yet to be found. There are also huge reserves of 'unconventional gas' in the form of methane hydrates (solids) most inaccessible to conventional drilling in deep water, the rest unstable.

2.1.2.3 Coal

Coal reserves are available in almost every country worldwide, with recoverable reserves in around 70 countries. The biggest reserves are in the USA, Russia, China and India. After centuries of mineral exploration, the location, size and characteristics of most countries' coal resources are quite well known. What tends to vary much more than the assessed level of the resource - i.e. the potentially accessible coal in the ground - is the level classified as proved recoverable reserves. Proved recoverable reserves is the tonnage of coal that has been proved by drilling etc. and is economically and technically extractable. Coal has been

the main fuel used for electrical power generation in the past. There is probably over 200years available supply in the world.

2.1.3 Energy Statistics of Bangladesh

Bangladesh having entered in the developing nation and trying to meet with the demands of the continuous developing world has a humongous need for energy. Every waking hour of the day and even at the middle of the night the need of energy is always there. Electricity production, industries operation, water extraction and purification, excavation, food manufacture all have a continuous requirement. As we are moving forward along with the rest of the world the requirement is continuously growing.

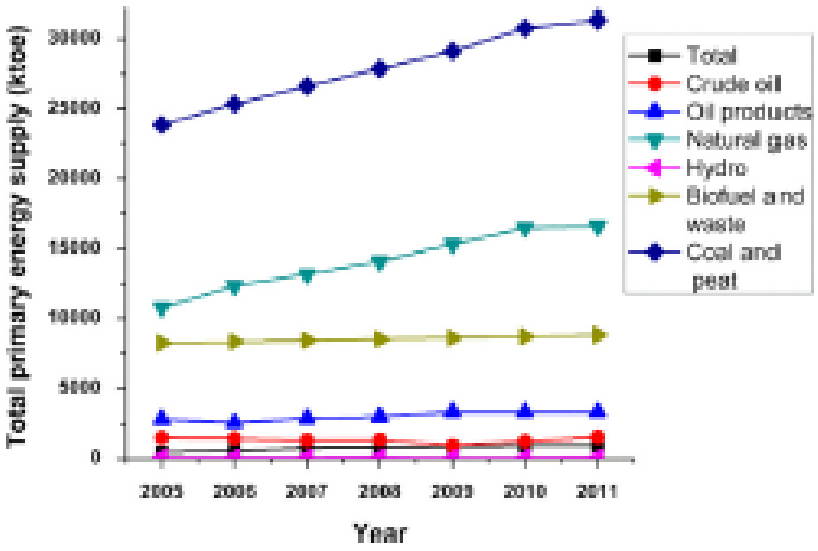

Figure 3 Energy Trend in Bangladesh over the years

2.1.4 Fuel Reserve and Consumption

2.1.4.1 Natural gas

Bangladesh's Ministry of Finance estimated in 2004 that the country holds 28.4 Tcf of total gas reserves, of which 20.5 Tcf is recoverable. In June 2001, the U.S. Geological Survey estimated that Bangladesh contains 32.1 Tcf of additional "undiscovered reserves."

In Bangladesh, natural gas is most important indigenous source of energy that accounts for 75% of the commercial energy of the country. So far in Bangladesh 23 gas fields have been

discovered. Gas is produced from 17 gas fields (79 gas wells).Oil was tested in two of the gas fields (Sylhet and Kailashtila).

2.1.4.2 Coal

Besides natural gas, Bangladesh has significant coal reserve. According to Bangladesh's National Energy Policy 2004 (quoted in The Independent, May 9) total coal reserves are 2,527 million tons, contained in four fields: Barapukuria with around 300 million tons; Phulbari with 400 million tons; Jamalganj containing 1,000 million tons, and 450 million tons at Khalaspir. Of these resources, 492 million tons are estimated to be recoverable by mining.

2.1.5 Fuel Reserve in Bangladesh

If we use constantly our natural resources of energy it is quite clear that after a few days the reserves will be set on a critical situation. As the Bangladesh develops rapidly, the energy demand follows. An increasing energy demand and the consequence of this increasing energy consumption is seen in climate changes all over the world as a reaction to the global warming due to the carbon dioxide emission and pollution.

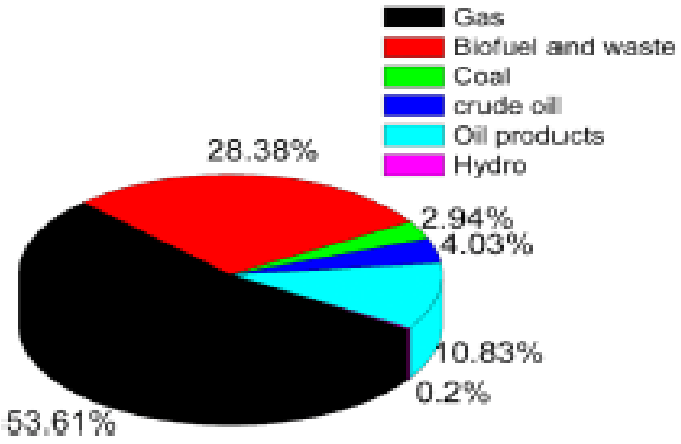

Figure 4 Energy Reserve in Bangladesh

The resources of fossil fuels (oil, coal, gas) are not unlimited, and the expected energy consumption for the future, these supplies will be emptied within the next generations. Therefore it is already now necessary to supplement and replace the fossil fuels with

renewable energy sources. Nuclear power, wind and hydro energy are strong players, but also solar energy is increasing. Especially the photovoltaic cells are of interest, as they convert solar energy to electricity which is a primary energy source.

2.1.6 Climate Change and Sustainable Development

We have all heard of acid rain, the Ozone layer and the Greenhouse Effect, but what exactly are they and how do they affect humans? Acid rain is caused by high concentrations of certain gases in the atmosphere. These high concentrations are the result of the emissions from the excessive burning of fossil fuel. Acid rain can cause fatal deterioration to field and forest regions. The ozone layer, considered the "protective shield" of life on Earth, regulates the amount of radiation that reaches Earth's surface. Because of the actions of humans, the ozone layer is deteriorating. The Greenhouse Effect produces rapid and alarming warming of the lower level atmosphere. It is caused by the presence of greenhouse gases (GHG) which trap heat that would otherwise escape into space.

The conjunction of these three phenomena will increase the number and intensity of catastrophic events, such as: floods, desertification, thaw, and ecosystem destruction. Additionally, the changes in climate patterns could create a food production crisis which would lead to a social crisis. Perhaps the most significant cause of the increased greenhouse effect and global warming is the 30% increase in atmospheric carbon dioxide (a well-known GHG) since 1750. Present carbon dioxide concentrations have not been seen in 20 million years. It is estimated that ¾ of the GHG emissions in the last 20 years is due to the burning of fossil fuels for human consumption and transportation. Today, one of society's primary concerns is moving from old development methods towards sustainable development.

Sustainable development methods are intended to satisfy current needs without compromising future generations. To ensure sustainable development, the corporate sector needs to work toward the objectives of Corporate Social Responsibility (CSR) and its stakeholders. In doing so, corporations would begin to manage their activities in a cleaner

and more efficient manner. The Kyoto Protocol, written in 1997, is an effort to work toward sustainable development. Although not signed by the USA, China or India, the Kyoto Protocol was signed by more than 55% of the countries worldwide. The goal of the Kyoto Protocol is to reduce the emissions levels of 6 major greenhouse gases in 1990 by 5.2% between the years 2008 and 2012. Only developed countries have been able to quantify their commitment to emissions reduction. Each developed country must distribute its emissions rights among its companies. If companies exceed their emissions rights they could be economically penalized. In the case that a company cannot viably remain under its emissions rights, flexible mechanisms have been created to help them comply with regulations. Within renewable, the potential of solar technologies has recently caused a large increase in its development. Flexible fostering mechanisms divided into: emissions trading, joint projects and clean development mechanisms that allow companies to receive emissions rights for investing in renewable energy (even if it is in another country).

Although the flexible fostering mechanisms that help companies comply with their emissions rights is good, it is undoubtedly better to avoid GHG pollution through the reduction or elimination of their emission. In order to do so we must use energy in a rational and efficient way and begin to integrate renewable energy technologies into our current systems.

2.1.7 Proposed Solution: Renewable Energy

Renewable energy technologies are those that provide energy from a source considered inexhaustible (i.e. the sun, wind, biomass, river water, etc.). The use of renewable energy technologies is an effective way to reduce emissions. Without initiatives to develop renewable energy technologies, today's total emissions would have increased by 30% above 1990 levels. Today, installed electricity capacity from renewable energy technology is 160 GW, which is 4% of the global installed electric capacity. Within renewable, the potential of solar technologies has recently caused a large increase in its development. Photovoltaic cells are now (since the oil crisis-marked 1970s) generally appreciated as a promising alternative to non-renewable energy sources. Dye Sensitized Solar Cells

(DSSCs) are subjects for scrutineers study worldwide. In the constantly evolving field of research of PEC cells, many discoveries are yet to be made. Lately, the solar-cell industry has grown swiftly. In 2001, the global energy production generated from photovoltaic (PV) cells surpassed 300 Megawatt (MW) and in 2003 it reached 740 MW. Silicon-based solar cells still dominate the PV energy market, holding roughly an 80% share of the present-day PV production. Predominant determinants in the fast growth in the PV energy production are a continuous decline of production costs and an increase of solar-cell efficiencies.

2.2 SOLAR ENERGY

Solar Energy is the ultimate source of energy. Every living being on earth is directly or indirectly dependent on solar energy. It is not only non-perishable but also the unique form of renewable energy. 99% of the solar energy is unused and lost every day. The application of such a magnitude of energy form is not only attractive but may also help mitigate all energy crisis of the world if proper application can be done.

2.2.1 Benefits of Solar Energy

One characteristics of the solar cell is that it is dependent on the availability of the irradiation. The characteristics of solar energy make it well suited to supply peak electricity demands. This is beneficial in a way since the requirement during summer increases and during midday increases. In the developed world the summer peak demands have become overwhelming and the winter peak demands are primarily due to space heating. When the solar radiation curve during the summer is analyzed, it is seen thatit coincides very closely with the peak power demand curve. This is very convenient because solar energy technologies can produce their maximum when the demand is at its maximum. Although they produce the most power during peak daylight hours, solar technologies can also be used to provide electricity throughout the day. By storing heat from solar radiation in

storage tanks and hybridizing with fossil fuels solar plants are able to provide clean and reliable electricity throughout the day. Solar technologies is becoming one of the foremost power sources worldwide due to its base and peak electricity demand meeting capability. The installation of solar plants is ideal in locations known as the "solar belt" (see picture). These locations in much of the world and receive high solar radiation. Over the last century, the financial investment in solar technology development has coincided with oil shortages. Due to increasing power consumption

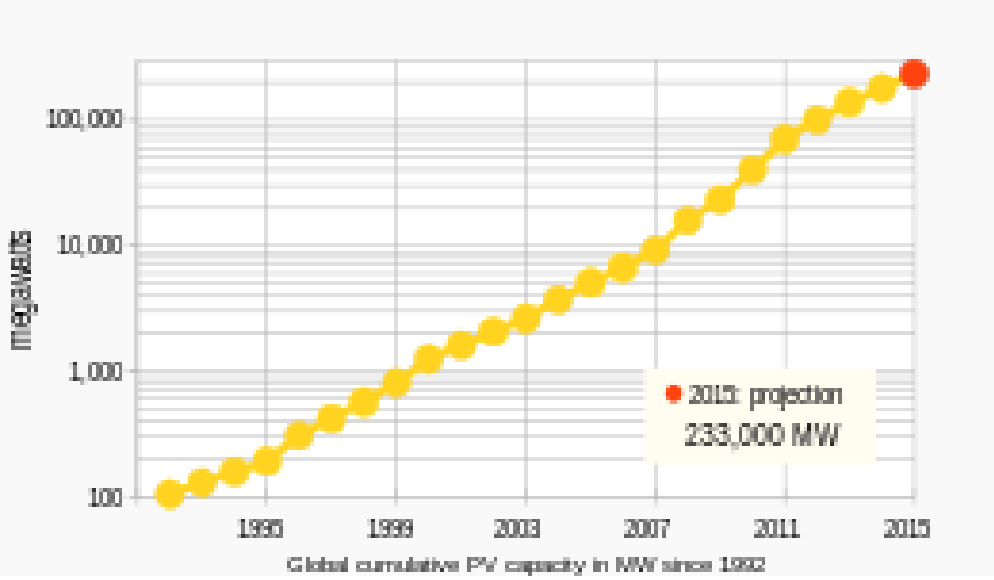

Figure 5 World Growth of Photovoltaic Cell over the Years

worldwide, the life expectancy of fossil fuels is dramatically shrinking. Experts' development due to increasing investment and an ever growing experience with the technology. "If only 2% of the solar radiation from the world's deserts were used it would be enough to supply the worlds power demands." Although energy from fossil fuels currently costs less than energy from renewable, concentrated solar power and photovoltaic technologies are predicted to cost less in the near future. Future power costs from fossil fuels will tend to increase due to increased demand and economic sanctions imposed on CO2 emissions.

2.2.2 Solar cell

A solar cell is a solid state electrical device that converts light energy directly into electricity by the photovoltaic effect, giving rise to the solar cell. Due the photovoltaic effect it is also known as photovoltaic cell or photoelectric cell.

The generation of electricity is mostly from visible light by means of the photovoltaic effect. Other wavelengths due to the heating effect and low generation of electricity from such waveengths is rejected. A solar cell generates small amount of power. In order to generate useful power, it is necessary to connect a number of cells together which forms a solar panel or the photovoltaic module, which in turn are connected together to form the photovoltaic array. The use of modules and arrays is to increase the required current and voltage to meet the demand.

Photovoltaics research and development will continue intense interest in new materials, cell designs, and novel approaches to solar material and product development. It is a future where the clothes you wear and your mode of transportation can produce power that is clean and safe. Technology roadmaps for the future outline the research and development path to full competitiveness of concentrating solar power (CSP) with conventional power generation technologies within a decade. The potential of solar power in the Southwest United States is comparable in scale to the hydropower resource of the Northwest. A desert area 10 miles by 15 miles could provide 20,000 megawatts of power, while the electricity needs of the entire United States could theoretically be met by a photovoltaic array within an area 100 miles on a side. Concentrating solar power, or solar thermal electricity, could harness the sun’s heat energy to provide large-scale, domestically secure, and environmentally friendly electricity.

The price of photovoltaic power will be competitive with traditional sources of electricity within 10 years. Solar electricity will be used to electrolyze water, producing hydrogen for fuel cells for transportation and buildings.

2.2.3 History of Solar Cell

Solar technology is not new technology. Its history spans from the 7th Century B.C. to today. We started out concentrating the sun's heat with glass and mirrors to light fires. Today, we have everything from solar-powered buildings to solar- powered vehicles. Here you can learn more about the milestones in the historical development of solar technology, century by century, and year by year. You can also glimpse the future. This timeline lists the milestones in the historical development of solar technology from the 7th Century B.C. to the 1200s A.D. There has been wide range of application of inorganic solar cell in the outerspace research and in power generation to meet the energy demands of different countries. However, thin film solar cell research and the organic research is still at its infant stage with promising scopes for improvements. The use of treatments, and other techniques to help improve cell efficiency is now at a good pace for the future scopes.

2.2.4 Types of Solar Cells

The performance of a solar or photovoltaic (PV) cell is measured in terms of its efficiency at converting sunlight into electricity. There are a variety of solar cell materials available, which vary in conversion efficiency.

2.2.4.1 Semiconductor Based Solar Cells

A solar cell consists of semiconductor materials the most popular of which is silicon, and still remains the most popular material for solar cells. Some of the types in which silicon is used are:

- Monocrystalline or single crystal silicon
- Multicrystalline silicon
- Polycrystalline silicon
- Amorphous silicon

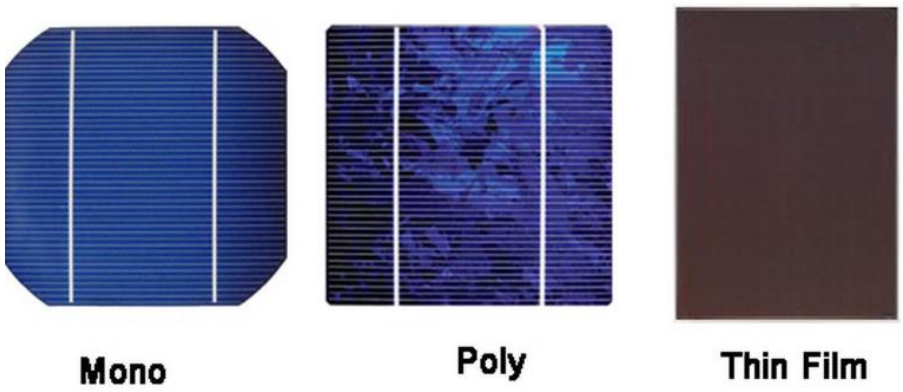

Figure 6 Different Types of Solar Cells

The absorption coefficient of a material indicates how far light with a specific wavelength (or energy) can penetrate the material before being absorbed. A small absorption coefficient means that light is not readily absorbed by the material. Again, the absorption coefficient of a solar cell depends on two factors: the material making up the cell, and the wavelength or energy of the light being absorbed.

The bandgap of a semiconductor material is an amount of energy. Specifically, the bandgap is the minimum energy needed to move an electron from its bound state within an atom to a free state. This free state is where the electron can be involved in conduction. The lower energy level of a semiconductor is called the "valence band." The higher energy level where an electron is free to roam is called the "conduction band." The bandgap (often symbolized by E_g) is the energy difference between the conduction band and valence band.

Solar cell material has an abrupt edge in its absorption coefficient; because light with energy below the material's bandgap cannot free an electron, it isn't absorbed.

2.2.5 Thin Film Solar Cell

Thin film solar cells use layers of semiconductor materials as thin as possible only a few micrometers thick making it more convinient for use. Thin film technology has made it possible for solar cells to now double as these materials provide extra features as:

- Rooftop or solar shingles
- Roof tiles
- Building facades
- Glazing for skylights or atria.

Attractive integration into homes, dual purpose—serves as both roofing material and pollution-free electricity producer and durability are some of the benefits that has made thin-film rooftop or solar shingles, made with various non-crystalline materials enter the residential market. Current issues with commercially-available solar shingles include their lower efficiencies and greater expense compared with the standard small solar electric system.

2.2.6 Dye sensitized solar cell

A dye-sensitized solar cell (abbreviated as DSSC, DSC or DYSC) is a low-cost solar cell belonging to the group of thin film solar cells. It is based on a semiconductor formed between a photo-sensitized anode and an electrolyte, a photo electrochemical system.

The dye solar cell, also known as the Grätzel cell, was invented by Michael Grätzel and Brian O'Regan at the École Polytechnique Fédérale de Lausanne in 1991. A world renowned invention and an alternative to the energy generation which has won Michael Grätzel the 2010 Millennium Technology Prize for phenomenal invention.

The DSC has the potential to be made from low-cost materials, when the use of noble materials like Platinum and Ruthenium is kept limited. The requirement of elaborate apparatus to manufacture, this cell is very low making it technically attractive. Likewise, manufacture can be significantly less expensive than older solid-state cell designs. It can also be engineered into flexible sheets and is mechanically robust, requiring no protection from minor events like hail or tree strikes. Although its conversion efficiency is less than the best thin-film cells, in theory its price/performance ratio (kWh/(m2·annum·dollar)) should be high enough to allow them to compete with fossil fuel electrical generation by achieving grid parity. Commercial applications ae soon expected to be present in the real world. In the late 1960s it was discovered that illuminated organic dyes can generate electricity at oxide electrodes in electrochemical cells.[7] In an effort to understand and simulate the primary processes in photosynthesis the phenomenon was studied at the University of Berkeley with chlorophyll extracted from spinach (bio-mimetic or bionic approach).[8] On the basis of such experiments electric power generation via the dye sensitization solar cell (DSSC) principle was demonstrated and discussed in 1972.[9] The instability of the dye solar cell was identified as a main challenge. Its efficiency could, during the following two decades, be improved by optimizing the porosity of the electrode prepared from fine oxide powder, but the instability remained a problem.[10] A modern DSSC, the Grätzel cell, is composed of a porous layer of titanium dioxide nanoparticles, covered with a molecular dye that absorbs sunlight, like the chlorophyll in green leaves. The titanium dioxide is immersed under an electrolyte solution, above which is a platinum-based catalyst. As in a conventional alkaline battery, an anode (the titanium dioxide) and a cathode (the platinum) are placed on either side of a liquid conductor (the electrolyte).

2.2.6.1 Evaluation of DSSC

- First Generation
    - Single crystal silicon wafers (c-Si)
- Second Generation
    - Amorphous silicon (a-Si)
    - Polycrystalline silicon (poly-Si)
    - Cadmium telluride (CdTe)
    - Copper indium gallium diselenide (CIGS) alloy
- Third Generation
    - Nanocrystal solar cells
    - Photo electrochemical (PEC) cells
    - Grätzel cells
    - Polymer solar cells
    - Dye sensitized solar cell (DSSC)

Chapter 3

3.1 LITERATURE REVIEW

Photovoltaic cellwas first discovered in the19th century, however practical photovoltaic devices made their first developed appearances in the 1950's using inorganic materials. The inorganic material, based on silicon, is used almost in all cases of production now-a-days. Some organic materials were found to have photovoltaic properties in the early 20th century while in the 1950s potential for PV cells were observed in polymers. Researches to find alternative energy sources were activated after the energy crisis that shook the world in the 1970s. Besides searching for new altenatives, researches to improve efficiencies and lower the production cost for inorganic photovoltaic cell had begun to make them commercially viable. The purification process for the silicon based photovoltaics shifted the focus of researchers towards organic photovoltaics. Despite a great deal of research, organic photovoltaics have yet to become practical.

Dye-sensitized solar cell use titanium dioxide as the semi-conductor while dye as the sensitizer. Most commonly used are the rhuthenium dye. The cost of inorganic dye being expensive ruthenium dye is preferrable. Researches have been performed to improve the cell conversion efficiency. Adsorpvity of the dye is important which depends on a number of factors, one of which is the acidity ogf the extracting solvent. The use of acidic environment to extract dye has proven to be positive in improving cell efficiency [1]. The cell current improvement is a major factor in defining an organic solar cell. The flow of current in the photovoltaic cell is dependent on the adsorpvity of the dye as it sensitizes more titanium dioxide molecules helping release more electrons. Iintramolecular push-pull system containing triphenylamine as the electron donor helps in adsoption of the dye and hence in current density of the cell [2]. The charge flow dynamics in the molecular orbitals (HOMO and LUMO levels)of molecules has effective role in charge separation which is an important feature of photosensitizers for DSSC [3].There has been an intensive search for a proper dye with high short-circuit current and open circuit voltage. The positive result hase been observed in terms of a number of materials. Although synthetic dye has proven to be better but the expense being high, alternative sources need to be looked for. Dye extracted from organic matter is relatively more affordable than synthetic dye. Starting from seed to different parts of full grown plants the search has benn wide. Anthrocyanin

containing plant leaves and fruits are preffered tfor high short circuit current[4][5]. Amongst other fruits black carrot and black berry dye extract meet the demands[4][5][6][7].

Dye extraction is an important step in cell fabrication. Using a solvent to extract the dye is a better idea than using raw dye as the dye for the cell. Beetroots, blackberries, black carrot and other anthrocyanin carrying fruits seem to release dye better in ethanol[4]. Acetone used as solvent has not proven to be positive although for most cases methon serves as better extracting solvent[4].

The main aim in DSSC fabrication is to improve the conversion effciency of the cell, for which improving short cicuit current density is vital. The use of a coating of blocking layer on the titanium dioxide paste is a remarkable technique. Titanium tetrachlride($TiCl_4$) treatment is a chemical technique to provide a layer over the titanium nanoparticles. The transparent layer over the nanocrystalline TiO_2 paste provides a photon-trapping layer to help in absorbing the photons in the titanium layer. Other techniques such as microcrystalline light-scattering layer in conjunction with the anti-reflecting film (ARF) are possible[4], however these techniques require additional instruments and are probably expensive. The results for the application of the $TiCl_4$ solution before and after the TiO_2 paste has been affirnmative in increasing the cell current and hence the incident photon and cell efficiency(IPCE). The treatment on the conductive glass electrodes, pre-treatment, and the treatment after, on the TiO_2 paste is post-treatment. Pre-treatment has the positive effect in helping the cell by reducing the emanating electrons from the the FTO and the I^{3-}ions, which originates from the I^{3-}/I^- redox couple[4][5]. The post treatment effect is still in controversy owing to the fact that there is already more than enough charge transport properties of the TiO_2 films without treatment. Hence improvements in charge transport is not justifiable to the increase in short circuit current density. However, researchers have come to a conclusion that the shift in conduction band edge, during the post treatment may be the result in improved charge injection into the TiO_2 layer[4].

3.2 AIM OF THE RESEARCH

This study focuses on analyzing the effect of treatments before and after the titanium dioxide paste application on the TCO glass. The pre and post treatment will be carried out with the natural dye, dye from blackberry, as the sensitizing agent.

- Pre ansd post treatment on titanium dioxide paste
- Complete Dye Sensitized Solar Cell fabrication using natural dye from blackberry
- Formulation and conditions to produce crystalline and conductive TiO_2 coating.
- Extracting and identifying highly efficient blackberry dye for the preparation of DSSC from natural resources.
- Construction and characterization of the prepared cell.

3.3 THEORY OF DYE SENSITIZED SOLAR CELL

Dye is the most important element in DSSC. The dye absorbs light energy to transfer from ground state to excited state and plays a role of electron injection. The DSSC-use dye must satisfy conditions as follows; first, it must be able to absorb lights from the entire visible ray field. Second, it must realize easy electron injection through fine chemical bond with nano oxide surface. Third, it must secure proper HOMO and LUMO energy levels and realize a molecule design which enables easy oxide semiconductor conduction band and charge mobility to be used. Fourth, it must secure thermal and optical stability and obtain about 108 degrees of oxidation-reduction turnover value which corresponds to 20 years of natural light. In addition, the light conversion efficiency reportedly becomes more outstanding as the lifetime of excited state elongates like the triplet state. Of dyes that are known thus far, ruthenium based organic metal compound reportedly is the most outstanding. DSSC's semiconductor electrode film is a nonconductor when there is no light, whereas the conduction increases when electrons are injected. The electron injection occurs through coexistence of two processes which mostly secure time constants of several tens of femto second and pico second. TiO_2 mainly occurs several femto seconds process.

By light, the electron moves from ruthenium to pyridine loop (dt2g→π*) and is again injected to π*(dt2g-O2p) orbital combined with $Ti^{4+}O^{2-}$. The fact that these two related orbitals secure equivalent symmetry enables easy injection process. Here, the quantum efficiency is generally over 90%. Katoh and others records such electron injection efficiency to nearly 100% in various semiconductors like TiO_2, ZnO, Nb_2O_5, In_2O_3, and SnO_2. However, the have revealed that ZrO_2, which has higher conduction band energy than LUMO of the dye, cannot realize the electron injection. Commonly, dye oxidation and conduction band electron formation processes are observed at 20 fs interval. This is analyzed to be extremely large injection speed constant of over $5\times1013s^{-1}$.

Such rapid electron delivery process cannot be explained by vibration-mediated electronic coupling which frequently appears in regular complex chemical process, but only by direct, strong electron coupling. In addition, this signifies that density of state which plays a role of conduction band internal acceptor is also important. On the other hand, a slower electron injection of pico seconds is observed for a case where dye is not ideally absorbed on the TiO_2 surface.

3.3.1 How Dye Sensitized Solar Cells Work

Sunlight enters the cell through the transparent glass, striking the dye on the surface of the TiO_2. Photons striking the dye with enough energy to be absorbed create an excited state of the dye, from which an electron can be "injected" directly into the conduction band of the TiO_2. From there it moves by diffusion (as a result of an electron concentration gradient) to the clear anode on top.

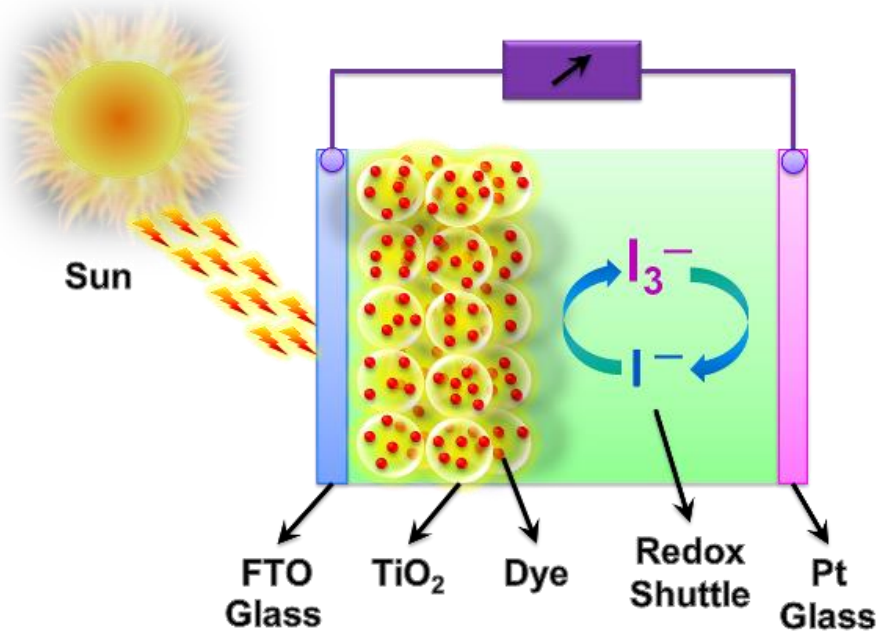

Figure 7 Mechanism of dye sensitized solar cell

Meanwhile, the dye molecule has lost an electron and the molecule will decompose if another electron is not provided. The dye strips one from iodide in electrolyte below the TiO_2, oxidizing it into triiodide. This reaction occurs quite quickly compared to the time that it takes for the injected electron to recombine with the oxidized dye molecule, preventing this recombination reaction that would effectively short-circuit the solar cell.

The triiodide then recovers its missing electron by mechanically diffusing to the bottom of the cell, where the counter electrode re-introduces the electrons after flowing through the external circuit.

- Dye molecules are hit by light
- Electrons in the dye are transmitted to TiO_2.
- The electrons are collected by front electrode and supplied to external load.
- Dye molecules are electrically reduced to their initial states by electrons transferred from redox couple in the electrolyte.

- The oxidized ions in the electrolyte, diffuse to the back electrode to receive electrons.

DSSC Reactions:

1. Dye excitation $E_{hv} + S \rightarrow S^*$
2. Electron injection $S^* \rightarrow e^- + S^+$
3. Dye regeneration $S^+ + A^- \rightarrow S + A$
4. Current collection $e^- + FTO \rightarrow e^1$
5. Electrolyte reduction $e^1 + A \rightarrow A^-$

The basic layout of the dye sensitized solar cell can be seen in figure 1. Two glass plates with conductive clear coating, usually Indium Tin Oxide (ITO) are used. Only one side of the glass is coated, so care must be taken to use the conductive side, which can easily be found by testing the resistivity with a multi-meter. The coated side shows measurable resistance, while the uncoated side has infinite resistance.

3.3.2 Three Main Components of dye sensitized solar cell

A layer of semiconductor is applied to one of the plates, making the cathode of the cell. Titanium dioxide (TiO_2) is used often, as this material is widely available and inexpensive. The application can be done in a number of two ways and the thickness is also controlled. This layer is then fired or sintered in such a way as to cause the TiO_2 to form crystals. An organic dye is applied to the cooled semi-conducting layer and allowed to dry. To create the anode, a layer of graphite is applied to the other glass plate, which serves to improve conductivity of that plate and as a catalyst for the electrochemical process. The plates are then put face-to-face with a liquate electrolyte solution between them. This is often an iodine/iodide solution, which readily exchanges electrons.

The dye molecules are chemically attached to the semi-conductive material. They do this by linking a complex sugar group known as Cyanin to one of the oxygen molecules in the TiO_2 crystal structure.

When the photon from the light source strike the dye, electrons in the dye become excited and are released into the semiconductor. From there they are free to flow through the semiconductor to the glass plate and out to the circuit. Once completing the circuit, they flow back to the anode, where the conductive graphite allows free flow of the electrons back through the electrolyte solution to the original site of the lost electron in the dye.

At its simplest configuration, the dye-sensitized solar cell (abbreviated here after as the DSSC or the dye cell) is comprised of a transparent conducting glass electrode coated with porous nano crystalline TiO_2 (nc-TiO_2), dye molecules attached to the surface of the nc-TiO_2, an electrolyte containing a reduction-oxidation couple such as I^-/I^{3-} and a catalyst coated counter-electrode. At the illumination the cell produces voltage over and current through an external load connected to the electrodes.

The absorption of light in the DSSC occurs by dye molecules and the charge separation by electron injection from the dye to the TiO_2 at the semiconductor electrolyte interface. A single layer of dye molecules however, can absorb only less than one percent of the incoming light (O'Regan & Grätzel 1991). While stacking dye molecules simply on top of each other to obtain a thick dye layer increases the optical thickness of the layer, only the dye molecules in direct contact to the semiconductor electrode surface can separate charges and contribute to the current generation. A solution to this problem, developed by the Grätzel group, was to use a porous nanocrystalline TiO_2 electrode structure in order to increase the internal surface area of the electrode to allow large enough amount of dye to be contacted at the same time by the TiO_2 electrode and the electrolyte. Having this construction, a TiO_2 electrode typically 10 mm thick, with an average particle (as well as pore) size typically in the order of 20 nm, has an internal surface area thousands of times greater than the geometrical (flat plate) area of the electrode, (O'Regan & Grätzel 1991). Essential to the optical operation of this porous electrode structure is the fact that TiO_2, as a large band gap semiconductor, absorbs only below

The incoming photon is absorbed by the dye molecule adsorbed on the surface on the nanocrystalline TiO_2 particle and an electron from a molecular ground state S0 is exited to a higher lying excited state S* (1). The exited electron is injected to the conduction band of the TiO_2 particle leaving the dye molecule to an oxidized state S+ (2). The injected

electron percolates through the porous nano crystalline structure to the transparent conducting oxide layer of the glass substrate (negative electrode, node) and finally through an external load to the counter-electrode (positive electrode, cathode) (3). At the counter-electrode the electron is transferred to triiodide in the electrolyte to yield iodine, and the cycle is closed by reduction of the oxidized dye by the iodine in the electrolyte.

I^-/ I^{3-} redox couple Wolfbauer et al. (2001) have listed the ideal characteristics of the redox couple for the DSSC electrolyte. Redox potential thermodynamically (energetically) favorable with respect to the redox potential of the dye to maximize cell voltage; High solubility to the solvent to ensure high concentration of charge carriers in the electrolyte; High diffusion coefficients in the used solvent to enable efficient mass transport; Absence of significant spectral characteristics in the visible region to prevent absorption of incident light in the electrolyte; High stability of both the reduced and oxidized forms of the couple to enable long operating life; Highly reversible couple to facilitate fast electron transfer kinetics; Chemically inert toward all other components in the DSSC.

Since the discovery of the DSSCs about ten years ago (O'Regan & Grätzel 1991) no redox couple preceding the performance of the I^-/ I^{3-} couple in the DSSC has been discovered (Wolfbauer et al. 2001). The I-/ I3- redox electrolyte is prepared by adding I2to the solvent together with some iodine salt such as KI (O'Regan & Grätzel 1991), LiI (Hagfeldt et al. 1994), alkyl methyl imidazolium iodide (Deb e al. 1998) and methyl-hexylimidazolium iodide MHImI (Chmiel et al. 1998). A recent report by Wolfbauer et al. (2001) clearly highlights the importance of the cation of the iodine salt to the performance of the DSSCs. The photocurrent output was found to increase linearly with decreasing cation radius, the smallest cations Li+ and K+ showing the best performance. The results also showed that the relative concentration of I3- to I-in the electrolyte is an important factor to the cell performance.

3.3.2.1 Advantages of dye sensitized solar cell

DSSCs are currently the most efficient third-generation (2005 Basic Research Solar Energy Utilization 16) solar technology available. Other thin-film technologies are

typically between 5% and 13%, and traditional low-cost commercial silicon panels operate between 12% and 15%. This makes DSSCs attractive as a replacement for existing technologies in "low density" applications like rooftop solar collectors, where the mechanical robustness and light weight of the glass-less collector is a major advantage. They may not be as attractive for large-scale deployments where higher-cost higher-efficiency cells are more viable, but even small increases in the DSSC conversion efficiency might make them suitable for some of these roles as well.

There is another area where DSSCs are particularly attractive. The process of injecting an electron directly into the TiO_2 is qualitatively different to that occurring in a traditional cell, where the electron is "promoted" within the original crystal. In theory, given low rates of production, the high-energy electron in the silicon could re-combine with its own hole, giving off a photon (or other form of energy) and resulting in no current being generated. Although this particular case may not be common, it is fairly easy for an electron generated in another molecule to hit a hole left behind in a previous photo excitation.

In comparison, the injection process used in the DSSC does not introduce a hole in the TiO_2, only an extra electron. Although it is energetically possible for the electron to recombine back into the dye, the rate at which this occurs is quite slow compared to the rate that the dye regains an electron from the surrounding electrolyte. Recombination directly from the TiO_2 to species in the electrolyte is also possible although, again, for optimized devices this reaction is rather slow. On the contrary, electron transfer from the platinum coated electrode to species in the electrolyte is necessarily very fast.

As a result of these favorable "differential kinetics", DSSCs work even in low-light conditions. DSSCs are therefore able to work under cloudy skies and non-direct sunlight, whereas traditional designs would suffer a "cutout" at some lower limit of illumination, when charge carrier mobility is low and recombination becomes a major issue. The cutoff is so low they are even being proposed for indoor use, collecting energy for small devices from the lights in the house.

A practical advantage, one DSSCs share with most thin-film technologies, is that the cell's mechanical robustness indirectly leads to higher efficiencies in higher

temperatures. In any semiconductor, increasing temperature will promote some electrons into the conduction band "mechanically". The fragility of traditional silicon cells requires them to be protected from the elements, typically by encasing them in a glass box similar to a greenhouse, with a metal backing for strength. Such systems suffer noticeable decreases in efficiency as the cells heat up internally. DSSCs are normally built with only a thin layer of conductive plastic on the front layer, allowing them to radiate away heat much easier, and therefore operate at lower internal temperatures.

3.3.2.2 Disadvantages of dye sensitized solar cell

The major disadvantage to the DSSC design is the use of the liquid electrolyte, which has temperature stability problems. At low temperatures the electrolyte can freeze, ending power production and potentially leading to physical damage. Higher temperatures cause the liquid to expand, making sealing the panels a serious problem. Another disadvantage is that costly ruthenium (dye), platinum (catalyst) and conducting glass or plastic (contact) are needed to produce the Grätzel cell. A third major drawback is that the electrolyte solution contains volatile organic compounds (or VOC's), solvents which must be carefully sealed as they are hazardous to human health and the environment. This, along with the fact that the solvents permeate plastics, has precluded large-scale outdoor application and integration into flexible structure.

Replacing the liquid electrolyte with a solid has been a major ongoing field of research. Recent experiments using solidified melted salts have shown some promise, but currently suffer from higher degradation during continued operation, and are not flexible.

Chapter 4

4.1 FABRICATION, EXPERIMENTATION AND CHARACTERIZATION TECHNIQUES

Fabrication of the dye sensitized solar cell is a simple and easy process. The use of conductive glasses (glass substrate with TCO layer on it) and available chemicals has made DSSC fabrication very low cost and available at hand. It is a mainly a five step process as is described below.

Step 1 : Development of the photo anode

Step 2 : Dyeing of the phoanode

Step 3 : Development of the counter elctrode

Step 4 : Combining the anode and counter electrodes face to face

Step 5 : Injecting electrolyte in between the two layers

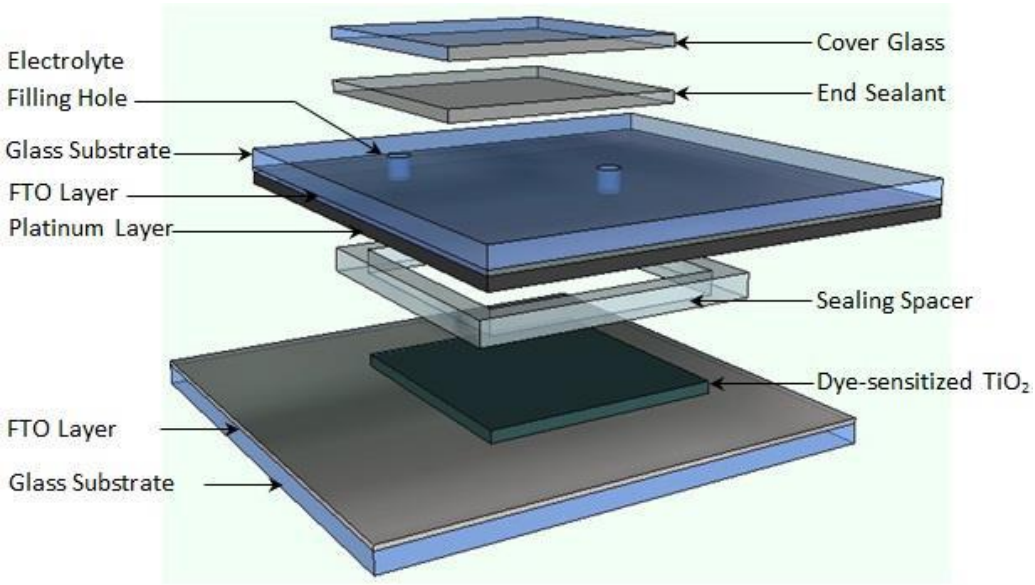

Figure 8 Layers of a Dye Sensitized Solar Cell

4.1.1 Materials required for fabrication:

- ITO(Indium doped Tin Oxide) glass (2 slides for 1 cell)- (Dye sol, Australia)
- TiO_2 (Degussa P25)
- Dye (Blackberry)
- Solvents ((Acetone (C_3H_6O), Ethanol (C_2H_6O), Methanol (CH_4O))- (Merck, Germany)
- Acetyl acetone - (Merck, Germany)
- Distill water
- Citric acid ($C_6H_8O_7$) - (Merck, Germany)
- Triton X 100 ($C_8H_{17}C_6H_4(OCH_2CH_2)_nOH$) - (Merck, Germany)
- Polyethylene glycol (PEG) - (Merck, Germany)
- Titanium tetrachloride ($TiCl_4$) - (Lobal Cheme Laboratory, India)
- Potassium iodide (KI)
- Iodine (I_2)
- Binder clips (small, 2 pieces for 1 cell)

Tools

- Hot plate
- Pipettes
- Tweezers
- Spatulas
- Scotch tape
- Electronic balance machine
- Ultrasonic cleaner - (Wincom)
- Multimeter - (HIOKI,3808 DIGITAL HiTESTER)
- Muffle Furnace - (Thermocon, India)
- UV- visible spectrometer - (T-60 UV- visible spectrometer, PG Electronics, UK)
- Scanning Electron Microscope (SEM) (EVO 18)
- Fourier Transform Infrared Spectroscopy (FTIR)

4.1.2 Fabrication of Dye Sensitized Solar Cell

4.1.2.1 Dye Extraction

In this study blackberry dye was used. For dye extraction the blackberries were washed properly with clean water to remove dust and dirt particles hence removing impurities. The berries were dried and then crushed in a clean dry mortar using a clean dry pestle as is shown in figure 8. The seeds were removed from the pulp during the crushing and care was taken while crushing the berries to prevent spillage of the juices from the berries.

Figure 9 Crushed blackberry for Dye extraction

The pulp were then taken in a clean dry beaker and soaked in solvent for extraction of the dye for 1 hour in a dark, dry place. In this study three different solvents (methanol, ethanol and acetone) were used, besides raw dye. In each of the three solvent cases after an hour and for the raw dye the pulp were then filtered using a clean piece of cloth to seperate the liquid from the pulp completely by squeezing the cloth as hard ar possible. The extracted liquid dyes were then filtered using a "Whatman Filter" before using the dye for staining the TiO_2 electrodes.

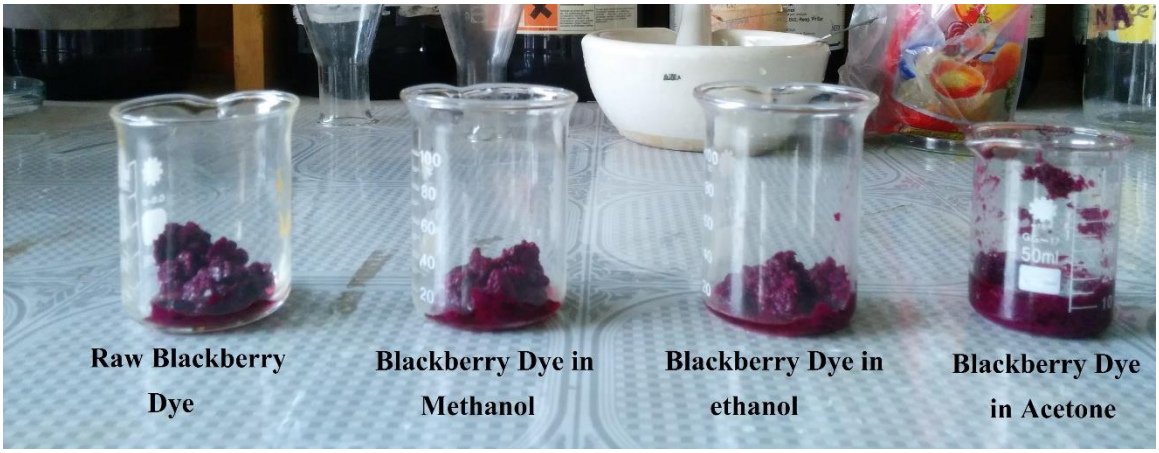

Figure 10 Crushed blackberry pulp immersed in solvents for extraction of dye

4.1.2.2 Preparation of TiO_2 paste

TiO_2 sol-gel paste was produced in the laboratory using nanocrystalline grade TiO_2 powder, anatase. A solution was prepared using 5ml of polyethylene glycol, 2.5ml of triton X-100, 50 ml of distill water and 1.25ml of acetyl acetone by stirring on a magnetic stirrer for 1 hour follwed by sonication in a probe sonicator for 15 minutes and further stirring for 1 hour.

Figure 11 Titanium dioxide paste preparation in a mortar

1.0gm of anatase powder is taken in a clean and dry mortar and 2ml of the above prepared solution was then added 1ml at a time to the for preparing the paste. The powder was mixed thoroughly to the solvent with a pestle to ensure the anatase powder is finely

grounded and a fine paste is prepared for coating. Thorough mixing is done by grinding the paste for around 5 minutes or by constantly checking until there is no visible powder particles.

4.1.2.3 Preparation of TiO_2 electrode (Cleaning and Coating of TCO glass)

4.1.2.3.1 Cleaning of the ITO glass slides

Clean dry ITO glasses were used in this research for the preparation of electrode.

The first step to cleaning is the washing of the glass slides using a cotton to rub detergent on the glass slides or by sonicating the slides in approximately 1gm of sodium dodecyl sulfate (detergent) in 250 ml of distill water for 10 minutes in a ultrasonic cleaner. The slides are then washed with distill water and placed in another beaker containing ethanol for further sonication for 10 minutes in an ultrasonic cleaner. The sides were then dried and conductive side were identified and with the conductive sides up were taped, by 1 mm from two edges, to the counter top using scotch tape.

4.1.2.3.2 Coating:

A glass rod is cleaned with athanol solution and distill water and dried. Using the pestle a small amount of TiO_2 paste, prepared previously, is placed on the slides. Using the glass

Figure 12 Applied TiO_2 paste on the ITO glass using glass

rod the paste is smeared evenly and as thin as possible on the glass slides such that the

thickness is approximately 0.2μm. This technique that have been followed for coating is the Doctor Blade technique.

The smeared paste is then allowed some time to dry before the tape is removed from the slides.

4.1.2.3.3 Annealing:

The glass slides are then cleaned of TiO_2 pastes from the edges and placed in a muffle furnace for an hour at 450 ˚C. Upon annealing the slides are allowed sufficient time to cool down to room temperature gradually. Drastic cooling or sudden drop in temperature will cause the coating on the slides to crack and also the bonding between TiO_2 particles will be affected. Hence care should be taken when the ITO glass slides are being taken out of the furnace.

Figure 13 Photoelectrode in a muffle furnace

4.1.2.3.4 $TiCl_4$ Treatment:

A blocking layer is provided on the electrode to help in improvement of the cells performance. This blocking layer is provided by the $TiCl_4$ treatment. This is a two step process:

1. $TiCl_4$ solution preparation:

For the blocking layer the solution preparation is the most crucial part. $TiCl_4$ is a highly explosive chemical and very cautious protective measures should be taken.

For the preparation of a 0.05M $TiCl_4$ solution, 0.56ml of $TiCl_4$ was added to 100ml of DI water. Care was taken while adding $TiCl_4$ to water.

The $TiCl_4$ container was placed in ice 5 minutes prior to adding to the already very chilled distill water in a beaker also placed in ice. Using a clean pipette 0.56ml of $TiCl_4$ was taken and added very slowly dropwise and along the walls of the beaker. The beaker containing the solution wa covered with parafilm and was then stirred on a magentic stirrer for 1 hour.

Figure 14 $TiCl_4$ solution being stirred on a stirrer.

2. Coating the electrode with the blocking layer

The substrates(ITO glasses)were then immersed in the freshly prepared $TiCl_4$ solution at 70˚C for 30 minutes. To maintain the temperature the Solution was placed in a water bath with the temperature kept constant at 70˚C.

After 30 minutes the electrodes were removed from the solution and then rinsed with deionised water followed by ethanol. It was then placed in a heater for 15 minutes at 80˚C to dry and finally sinistered at 500˚C for 10 minutes. When cooled back to room temperature the electrode is ready to be immersed in dye solution.

Figure 15 Water bath to maintain continuous temperature while coating.

4.1.2.3.5 Dyeing:

The electrode was then placed in the dye, extracted using the earlier method, for an hour. This container was then placed in a dark place away from light. The TiO_2/dye electrode is then removed from the dye solution and washed fresh respective solvent to remove excess liquid. Distill water is used for raw dye. The final step is to allow the electrodes to dry at room temperature.

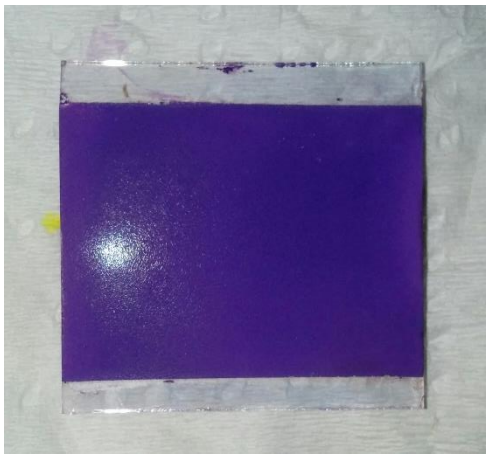

Figure 16 A photoelectrode dyed with blackberry dye.

4.1.2.4 Preparation of electrolyte

The electrolyte used in the DSSCs consists of iodine (I-) and triiodide (I3-) as a redox couple in a solvent with chemicals added to improve the properties of the electrolyte and the performance of the operating DSSC.

For the preparation of Iodide electrolyte solution, 0.05M 0.064g Iodine (I2) was dissolved in 10 mL of ethylene glycol followed by0.5M 0.83 g Potassium Iodide (KI). The solution is then stirred and stores in a dark container away from light.

4.1.2.5 Counter electrode

The counter electode used in this research is the the carbon elecrode prepared from candle flame. For the preparation of counter electrode a clean, dry ITO glass with the conductive side identified and facing downwards towards the flame was held by the help of tweezers on top of the tip of a candle flame. The carbon soot from the flame gets deposited on the conductive side of the glass. The glass slide was moved around so that there was even deposition of the soot all over the slide. Care was taken while working with the flame and when placing the slide aside since the soot is very light and is removed easily by touch. The slide is left aside with the soot face facing upwards, ready for assembly.

Figure 17 A counter electrode.

4.1.3 Characterization of prepared samples

4.1.3.1 Characteristic curves

There are basically two types of characteristics to compare and understand the performance of a electrical device.

1. I-V charateristic curve
2. P-V characteristic curve

The **I-V Characteristic Curves**, which is short for **Current-Voltage Characteristic Curves** or simply **I-V curves** of an electrical device or component, are a set of graphical curves which are used to define its operation within an electrical circuit. As its name suggests, I-V characteristic curves show the relationship between the current flowing through an electronic device and the applied voltage across its terminals.

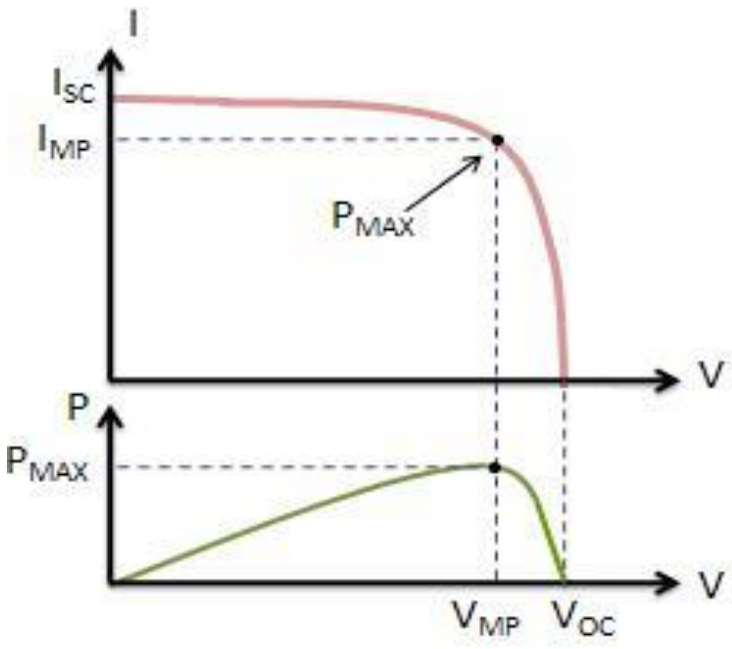

Figure 18 Ideal I-V and P-V Characteristic Curve

The **P-V Characteristic Curves**, which is short for **Power-Voltage Characteristic Curves** or simply **P-V curves** of an electrical device or component, are a set of graphical curves which are used to define its operation within an electrical circuit. As its name suggests, P-V characteristic curves show the relationship between the power generated by an electronic device and the applied voltage across its terminals.

The I-V (current-voltage) curve of a PV string (or module) describes its energy conversion capability at the existing conditions of irradiance (light level) and temperature. Conceptually, the curve represents the combinations of current and voltage at which the string could be operated or 'loaded', if the irradiance and cell temperature could be held constant. The span of the I-V curve ranges from the short circuit current (I_{sc}) at zero volts, to zero current at the open circuit voltage (V_{oc}). At the 'knee' of a normal I-V curve is the maximum power point (I_{mp}, V_{mp}), the point at which the array generates maximum electrical power. In an operating photovoltaic (PV) system, one of the jobs of the inverter is to constantly adjust the load, seeking out the particular point on the I-V curve at which the array as a whole yields the greatest DC power. At voltages well below Vmp, the flow of solar-generated electrical charge to the external load is relatively independent of output voltage. Near the knee of the curve, this behavior starts to change. As the voltage increases further, an increasing percentage of the charges recombine within the solar cells rather than flowing out through the load. At V_{oc}, all of the charges recombine internally. The maximum power point, located at the knee of the curve, is the (I, V) point at which the product of current and voltage reaches its maximum value.

4.1.3.1.1 Resistance

The electrical resistance of a circuit component or device is defined as the ratio of the voltage applied to the electric current which flows through it:

$$I = V/R$$

If the resistance is constant over a considerable range of voltage, then Ohm's law, I = V/R, can be used to predict the behavior of the material. Although the definition above involves DC current and voltage, the same definition holds for the AC application of resistors.

Whether or not a material obeys Ohm's law, its resistance can be described in terms of its bulk resistivity. The resistivity, and thus the resistance, is temperature dependent. Over sizable ranges of temperature, this temperature dependence can be predicted from a temperature coefficient of resistance.

Morphological Analysis of the Surface

4.1.3.1.2 Scanning Electron Microscopy (SEM)

The scanning electron microscope (SEM) uses a focused beam of high-energy electrons to generate a variety of signals at the surface of solid specimens. The signals that derive from electron-sample interactions reveal information about the sample including external morphology (texture), chemical composition, and crystalline structure and orientation of materials making up the sample. In most applications, data are collected over a selected area of the surface of the sample, and a 2-dimensional image is generated that displays spatial variations in these properties. Areas ranging from approximately 1 cm to 5 microns in width can be imaged in a scanning mode using conventional SEM techniques (magnification ranging from 20X to approximately 30,000X, spatial resolution of 50 to 100 nm). The SEM is also capable of performing analyses of selected point locations on the sample; this approach is especially useful in qualitatively or semi-quantitatively determining chemical compositions (using EDS), crystalline structure, and crystal orientations (using Electron Backscatter Diffraction or EBSD).

To investigate the morphology of the pure TiO_2 in this study, SEM (scanning electron microscopy) images were obtained using a SEM instrument (Carl Zeiss EVO 18) equipped with energy dispersive spectroscopic (EDS) microanalysis system. Bulk EDS analysis was also performed to verify the elemental composition of the deposited materials on the fiber surface. It essential features being resolution: 3nm@30kV HV mode; 10nm @3 kV HV mode, detectors: Secondary Electron; Semiconductor BSE (Quad type)*, magnification: 5x to 300,000x; vacuum System: TMP & Rotary to 1.5 x 10^{-3} Pa, specimen height: 80mm at 10mm W.D.

4.1.3.1.3 UV-VIS Spectroscopy Analysis

A beam of light from a visible and/or UV light source (colored red) is separated into its component wavelengths by a prism or diffraction grating. Each monochromatic (single wavelength) beam in turn is split into two equal intensity beams by a half-mirrored device. One beam, the sample beam (colored magenta), passes through a small transparent container (cuvette) containing a solution of the compound being studied in a transparent solvent. The other beam, the reference (colored blue), passes through an identical cuvette containing only the solvent. The intensities of these light beams are then measured by electronic detectors and compared. The intensity of the reference beam, which should have suffered little or no light absorption, is defined as I0. The intensity of the sample beam is defined as I. Over a short period of time, the spectrometer automatically scans all the component wavelengths in the manner described. The ultraviolet (UV) region scanned is normally from 200 to 400 nm, and the visible portion is from 400 to 800 nm.

If the sample compound does not absorb light of a given wavelength, I = I0. However, if the sample compound absorbs light then I is less than I0, and this difference may be plotted on a graph versus wavelength, as shown on the right. Absorption may be presented as transmittance (T = I/I0) or absorbance (A= log I0/I). If no absorption has occurred, T = 1.0 and A= 0. Most spectrometers display absorbance on the vertical axis, and the commonly observed range is from 0 (100% transmittance) to 2 (1% transmittance). The wavelength of maximum absorbance is a characteristic value, designated as λ_{max}. Different compounds may have very different absorption maxima and absorbance. Intensely absorbing compounds must be examined in dilute solution, so that significant light energy is received by the detector, and this requires the use of completely transparent (non-absorbing) solvents. The most commonly used solvents are water, ethanol, hexane and cyclohexane. Solvents having double or triple bonds, or heavy atoms (e.g. S, Br & I) are generally avoided. Because the absorbance of a sample will be proportional to its molar concentration in the sample cuvette, a corrected absorption value known as the molar absorptivity is used when comparing the spectra of different compounds.

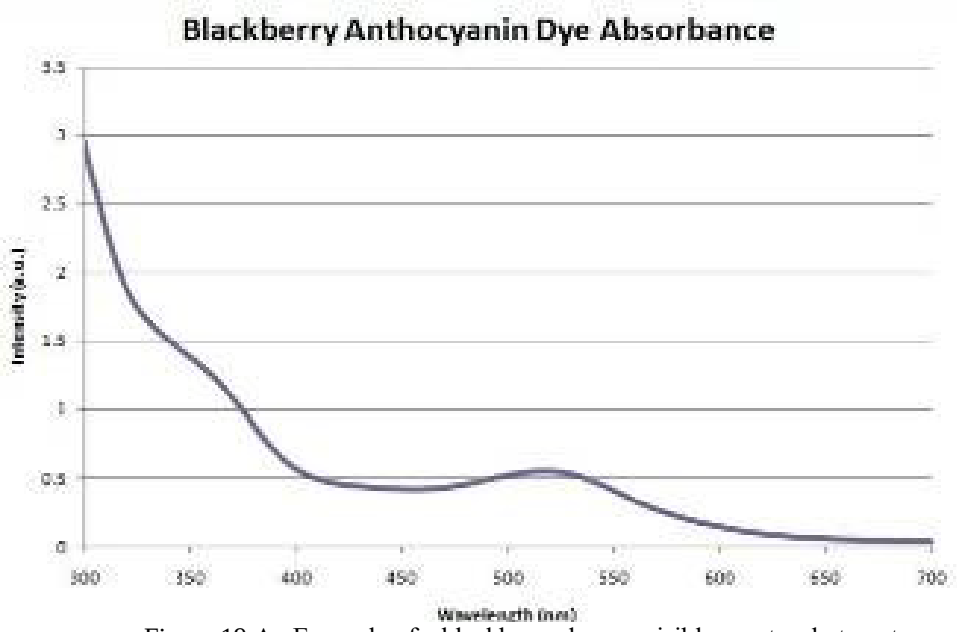

Figure 19 An Example of a blackberry dye uv-visible spectrophotometry

4.1.3.1.4 FTIR Spectroscopy Analysis

FT-IR stands for Fourier Transform Infrared, the preferred method of infrared spectroscopy. In infrared spectroscopy, IR radiation is passed through a sample. Some of the infrared radiation is absorbed by the sample and some of it is passed through (transmitted). The resulting spectrum represents the molecular absorption and transmission, creating a molecular fingerprint of the sample. Like a fingerprint no two unique molecular structures produce the same infrared spectrum. This makes infrared spectroscopy useful for several types of analysis.

Similar to ultraviolet-visible ("UV-Vis") spectroscopy the goal of FTIR spectroscopy is to measure how well a sample absorbs light at each wavelength. The most straightforward way to measure the absorption spectrum is to shine a monochromatic light beam at a sample, measure how much of the light is absorbed, and repeat for each different wavelength. Fourier transform spectroscopy is a less intuitive way to obtain the same information. Rather than shining a monochromatic beam of light at the sample, this technique shines a beam containing many frequencies of light at once, and measures how much of that beam is absorbed by the sample. Next, the beam is modified to contain a

different combination of frequencies, giving a second data point. This process is repeated many times. Afterwards, a computer takes all these data and works backwards to infer what the absorption is at each wavelength.

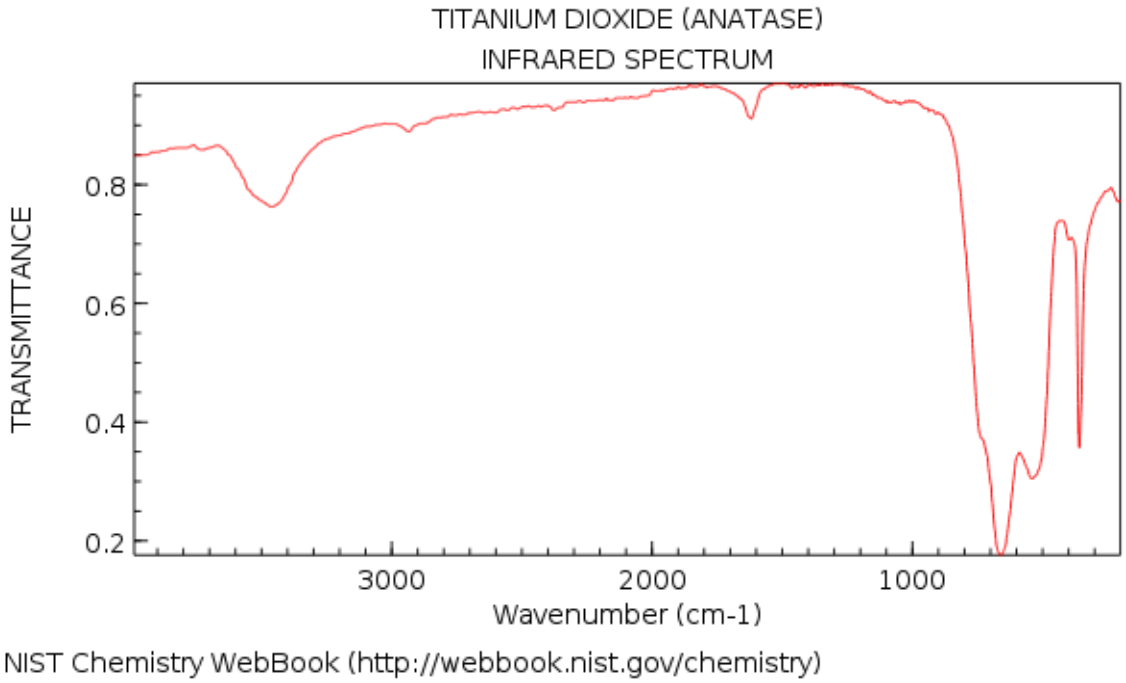

Figure 20 Expected FTIR from TiO_2

Chapter 5

5.1 RESULTS AND DISCUSSION

5.1.1 Experimental data, I-V and P-V Characteristic Curve

5.1.1.1 Raw blackberry:

A cell of the area 3.74cm^2 was fabricated using raw blackberry dye and was chracterized at an input power of 1000W. The resulting current through the cell and the voltage across the cell was obtained to develop a IV and PV-curve which is shown in figure 21 and figure 22 respectively. The span of the I-V curve ranges from the short circuit current (I_{sc}= 0.6mA) at zero volts, to zero current at the open circuit voltage (V_{oc}=440mV). The current almost stays constant with a slight decrease as the voltage increases. At the 'knee' of the I-V curve is the maximum power point (I_{mp}, V_{mp}), which are I_{mp}= 0.455mA and V_{mp}= 265mV and generates maximum electrical power of 120.575mW. Beyond the knee of the curve, this behavior starts to change as the current starts to fall sharply with increasing voltage. The efficiency and the fill-factor were calculated and found to be 0.0322% and 0.456 respectively. The J_{sc} was 0.121mA/cm^2. The knee of this curve is not very sharp since the range of data was not enough and the efficiency is low due a number of factors including impurites in raw dye and less soaking time of the electrode.

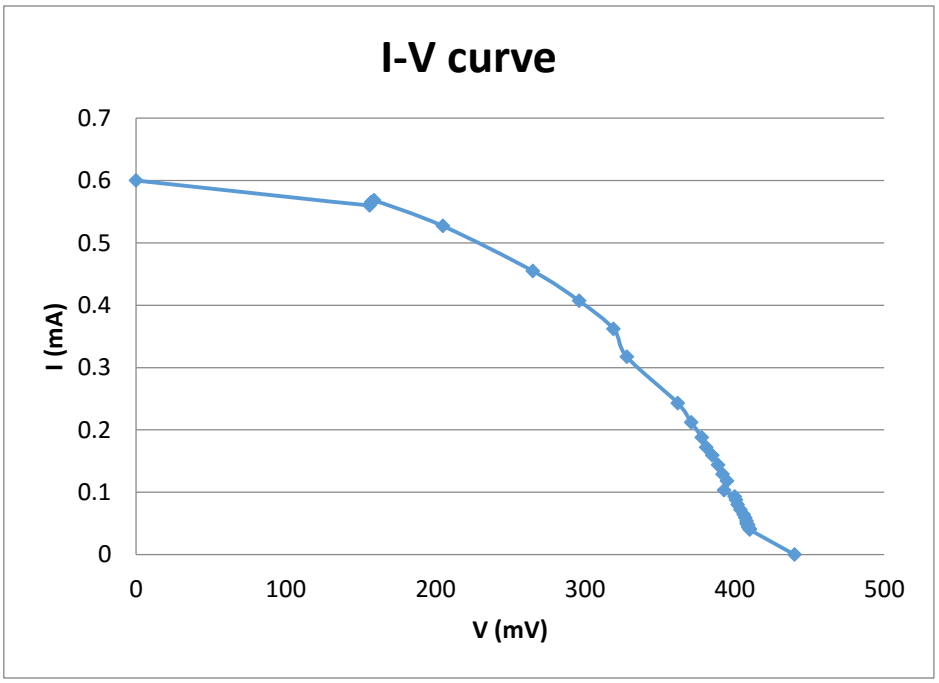

Figure 21 I-V Curve of raw dye fabricated cell

From the PV-curve we can see the highest peak of the curve is 120.575mW at a voltage of 0.455mV. The bell shaped curve gives the idea that as there is increase in voltage the power generating ability of the cell increases although it is till a certain limit. Beyond the peak point the power generation decreases due to internal losses involved.

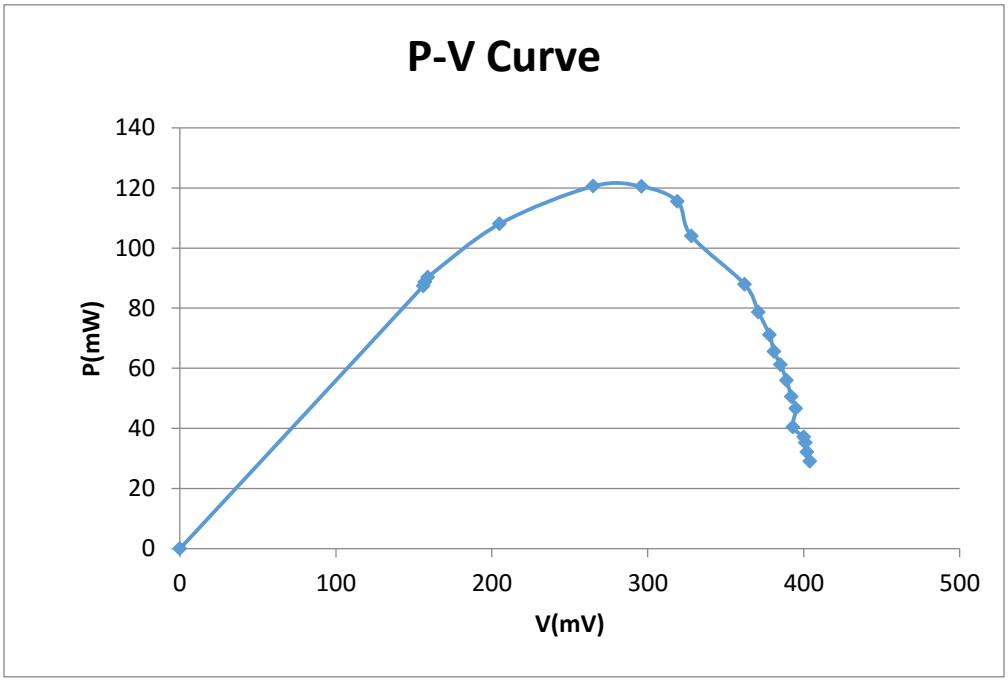

Figure 22 P-V Curve of raw dye fabricated cell

5.1.1.2 Ethanol

A cell of the area 3.74cm^2 was fabricated using blackberry dye in ethanol and was chracterized at an input power of 1000W. The resulting current through the cell and the voltage across the cell was obtained to develop a IV and PV-curve which is shown in figure 23 and figure 24 respectively. The span of the I-V curve ranges from the short circuit current (I_{sc}= 0.943mA) at zero volts, to zero current at the open circuit voltage (V_{oc}=497mV). The current almost stays constant with a slight decrease as the voltage increases. At the 'knee' of the I-V curve is the maximum power point (I_{mp}, V_{mp}), which are I_{mp}= 0.62mA and V_{mp}= 307mV and generates maximum electrical power of 190.34mW. Beyond the knee of the curve, this behavior starts to change as the current starts to fall sharply with increasing voltage. The efficiency and the fill-factor were calculated and found to be 0.0509% and 0.406 respectively. The J_{sc} was 0.166mA/cm^2.

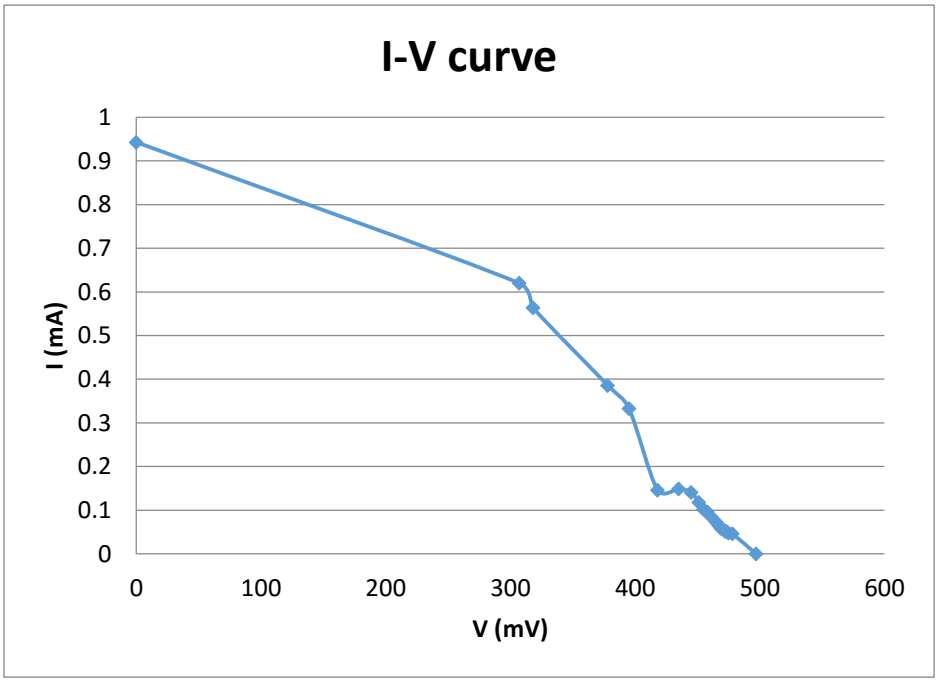

Figure 23 I-V Curve of a fabricated cell using ethanol soaked blackberry dye

From the PV-curve we can see the highest peak of the curve is 190.34mW at a voltage of 307mV. The bell shaped curve gives the idea that as there is increase in voltage the power generating ability of the cell increases although it is till a certain limit. Beyond the peak point the power generation decreases due to internal losses involved.

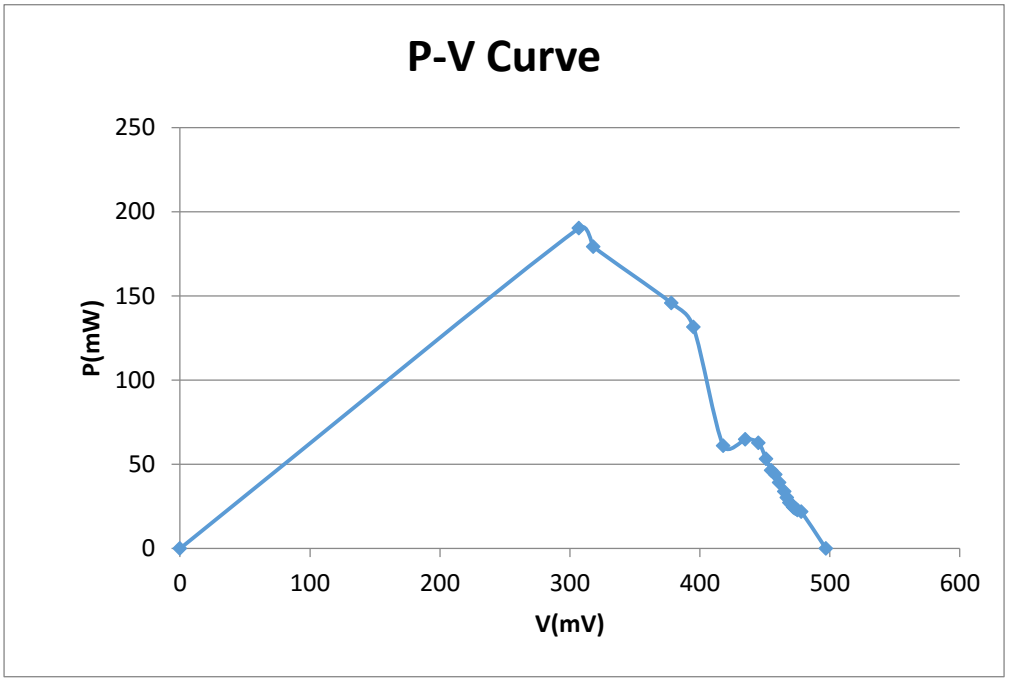

Figure 24 P-V Curve of a fabricated cell using ethanol soaked blackberry dye

5.1.1.3 Acetone

A cell of the area 4.25cm^2 was fabricated using blackberry dye in acetone and was chracterized at an input power of 1000W. The resulting current through the cell and the voltage across the cell was obtained to develop a IV and PV-curve which is shown in figure 25 and figure 26 respectively. The span of the I-V curve ranges from the short circuit current (I_{sc}= 0.7mA) at zero volts, to zero current at the open circuit voltage (V_{oc}=550mV). The current almost stays constant with a slight decrease as the voltage increases. At the 'knee' of the I-V curve is the maximum power point (I_{mp}, V_{mp}), which are I_{mp}= 0.45mA and V_{mp}= 283mV and generates maximum electrical power of 127.35mW. Beyond the knee of the curve, this behavior starts to change as the current starts to fall sharply with increasing voltage. The efficiency and the fill-factor were calculated and found to be 0.0299% and 3.31 respectively. The J_{sc} was 0.0165A/cm^2.

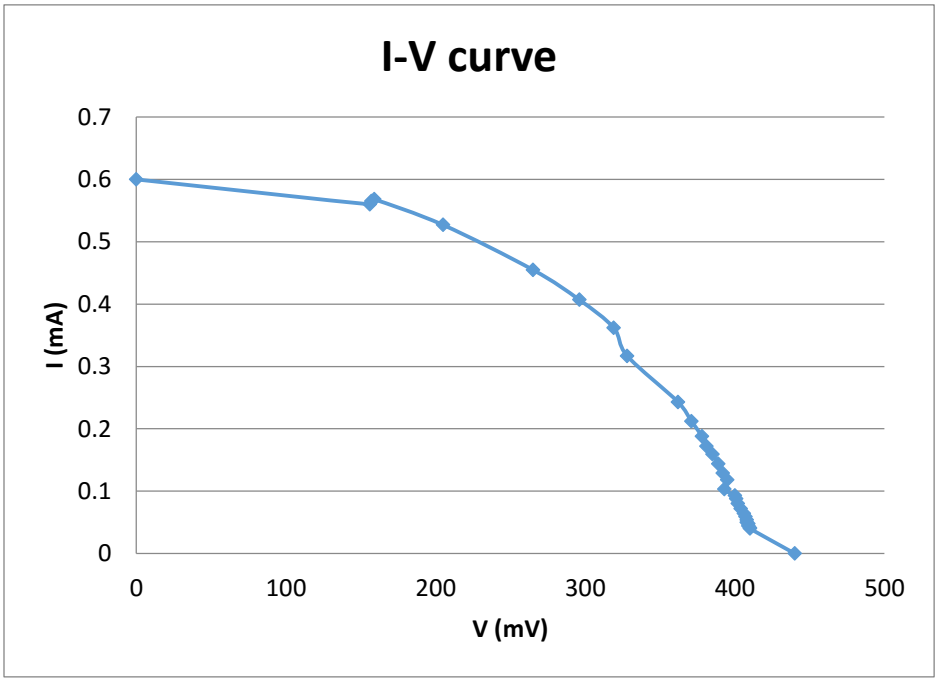

Figure 25I-V Curve of a fabricated cell using acetone soaked blackberry dye

From the PV-curve we can see the highest peak of the curve is 127.35mW at a voltage of 283mV. The bell shaped curve gives the idea that as there is increase in voltage the power generating ability of the cell increases although it is till a certain limit. Beyond the peak point the power generation decreases due to internal losses involved.

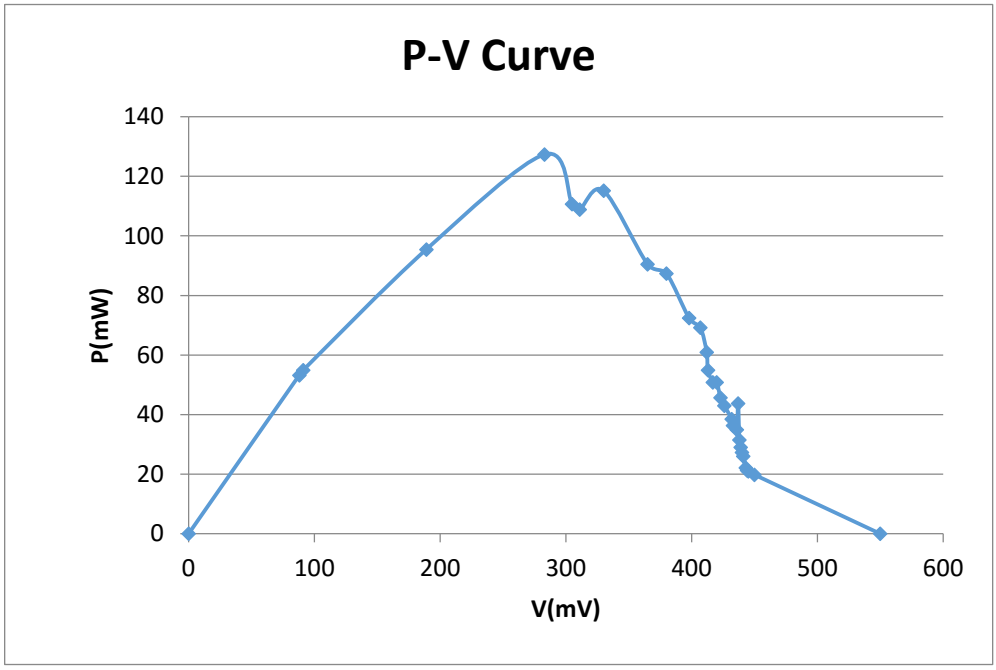

Figure 26P-V Curve of a fabricated cell using acetone soaked blackberry dye

5.1.1.4 Post treatment 70 degrees

A cell of the area 5.5cm^2 was fabricated using blackberry dye in ethanol with post treatment performed on the TiO_2 layer before application of dye. The treatment was done by immersing the photelectrode in $TiCl_4$ at 70˚. The cell was characterized at an input power of 1000W. The resulting current through the cell and the voltage across the cell was obtained to develop a IV and PV-curve which is shown in figure 27 and figure 28 respectively. The span of the I-V curve ranges from the short circuit current (I_{sc}= 1.5mA) at zero volts, to zero current at the open circuit voltage (V_{oc}=453mV). The current almost stays constant with a slight decrease as the voltage increases. At the 'knee' of the I-V curve is the maximum power point (I_{mp}, V_{mp}), which are I_{mp}= 1.387mA and V_{mp}= 342mV and generates maximum electrical power of 474.354mW. Beyond the knee of the curve, this behavior starts to change as the current starts to fall sharply with increasing voltage. The efficiency and the fill-factor were calculated and found to be 0.086% and 0.695 respectively. The J_{sc} was 0.274mA/cm^2. The knee of this curve is not very sharp since the range of data was not enough and the efficiency is low due a number of factors including impurites in raw dye and less soaking time of the electrode.

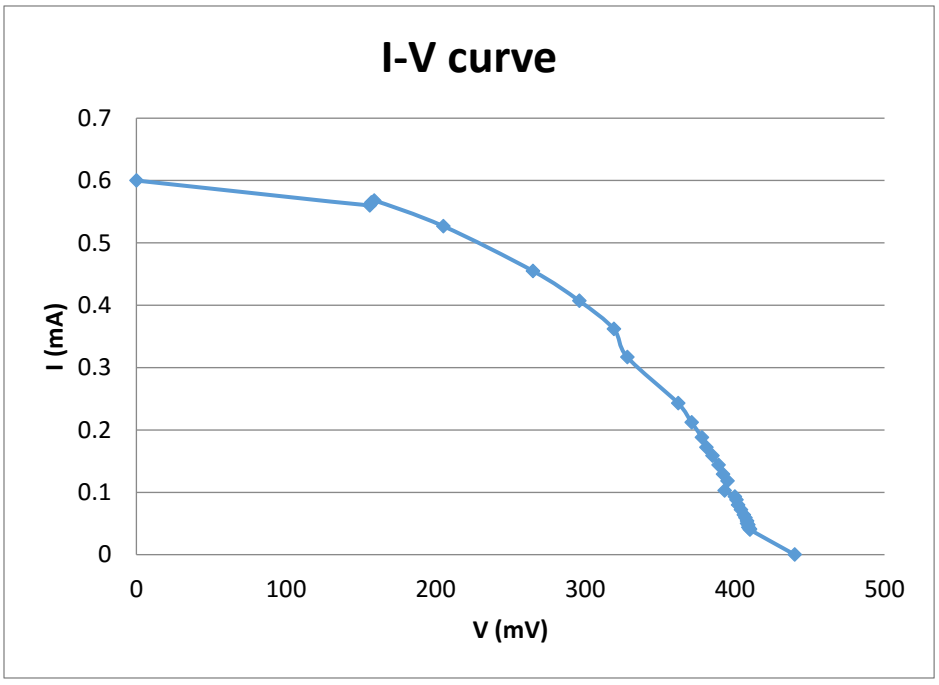

Figure 27 I-V Curve of a post treated (at 70 degrees) fabricated cell using ethanol soaked blackberry dye

From the PV-curve we can see the highest peak of the curve is 190.34mW at a voltage of 0.307mV. The bell shaped curve gives the idea that as there is increase in voltage the power generating ability of the cell increases although it is till a certain limit. Beyond the peak point the power generation decreases due to internal losses involved.

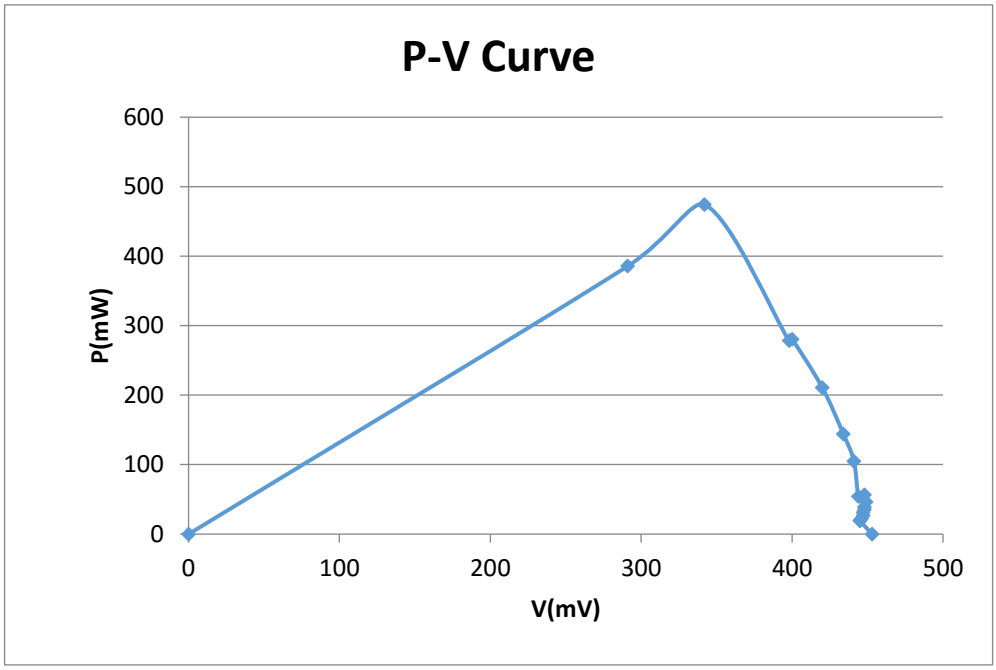

Figure 28 P-V Curve of a post treated (at 70 degrees) fabricated cell using ethanol soaked blackberry dye

5.1.1.5 Post treatment 12 hours

A cell of the area 4.25cm^2 fabricated using blackberry dye in ethanol with post treatment performed on the TiO_2 layer before application of dye. The treatment was done by immersing the photelectrode in $TiCl_4$ and stored in the refrigerator for 12 hours . The cell was characterized at an inputan input power of 1000W. The resulting current through the cell and the voltage across the cell was obtained to develop a IV and PV-curve which is shown in figure 29 and figure 30 respectively. The span of the I-V curve ranges from the short circuit current (I_{sc}= 0.976mA) at zero volts, to zero current at the open circuit voltage (V_{oc}=480mV). The current almost stays constant with a slight decrease as the voltage increases. At the 'knee' of the I-V curve is the maximum power point (I_{mp}, V_{mp}), which are I_{mp}= 0.319mA and V_{mp}= 68mV and generates maximum electrical power of 21.69mW. Beyond the knee of the curve, this behavior starts to change as the current starts to fall sharply with increasing voltage. The efficiency and the fill-factor were calculated and found to be 0.0051% and 0.0463 respectively. The J_{sc} was 0.229mA/cm^2. The knee of this curve is not very sharp since the range of data was not enough and the efficiency is low due a number of factors.

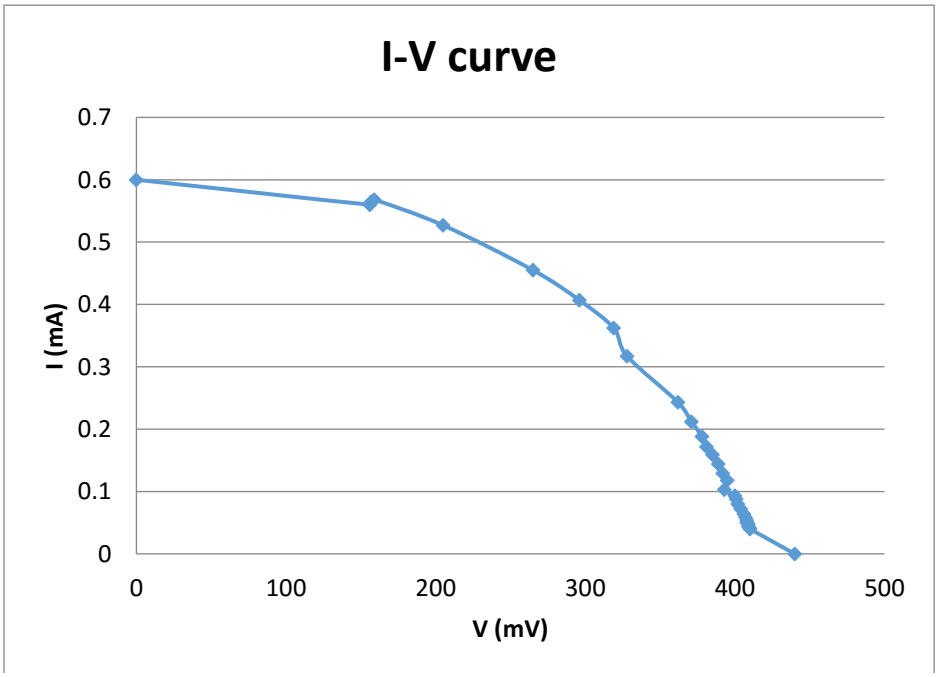

Figure 29 I-V Curve of a post treated (for 12hours) fabricated cell using ethanol soaked blackberry dye

From the PV-curve we can see the highest peak of the curve is 21.69mW at a voltage of 68mV. The bell shaped curve gives the idea that as there is increase in voltage the power generating ability of the cell increases although it is till a certain limit. Beyond the peak point the power generation decreases due to internal losses involved.

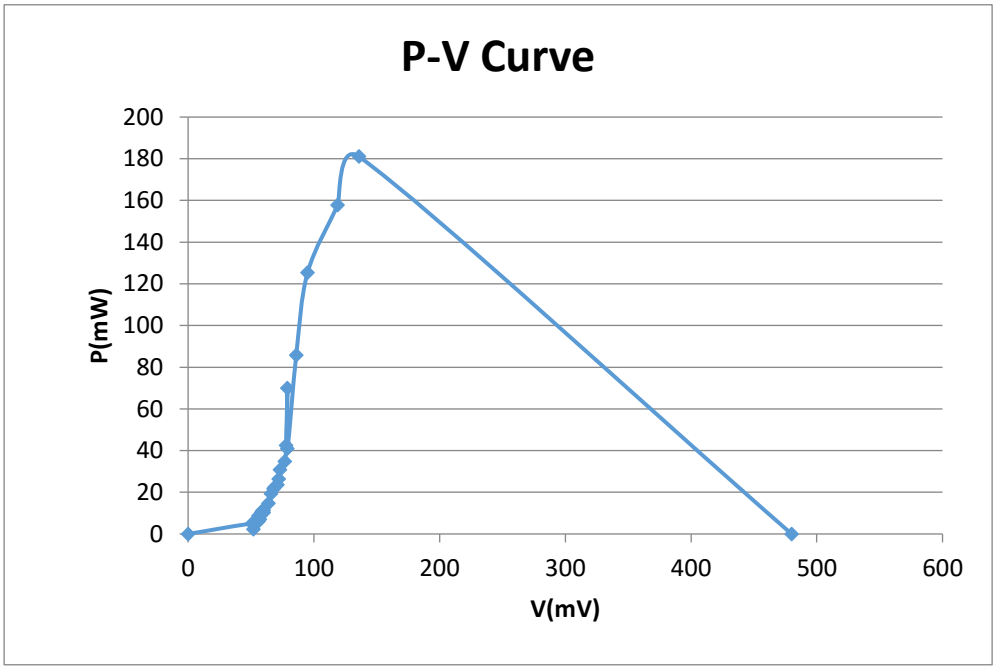

Figure 30 I-V Curve of a post treated (for 12 hours) fabricated cell using ethanol soaked blackberry dye

It is seen clearly that in each of the case with or without post treatment the IV-Curve does not have a prominent knee. This deviation is because there is a lot of internal losses. The I_{sc} increases because of less charge recombination taking place. Since there is still charge recombination taking place, there us a trend of I_{sc} decreasing and hence effecting power.

5.1.2 SEM Results

It was found that sample showed uniform crystalline nano structure with evenly distributed pores ranged 900-1000 nm. No distinguishable change was found between the samples with dye and without dye. Both the samples showed rough surfaces which may be formed due to uneven manual coating. These rough surfaces probably responsible for increased electrical resistance resulting reduced efficiency. It can be assumed that same formulation will produce cells with higher efficiency if coated by a precise automatic coating machine.

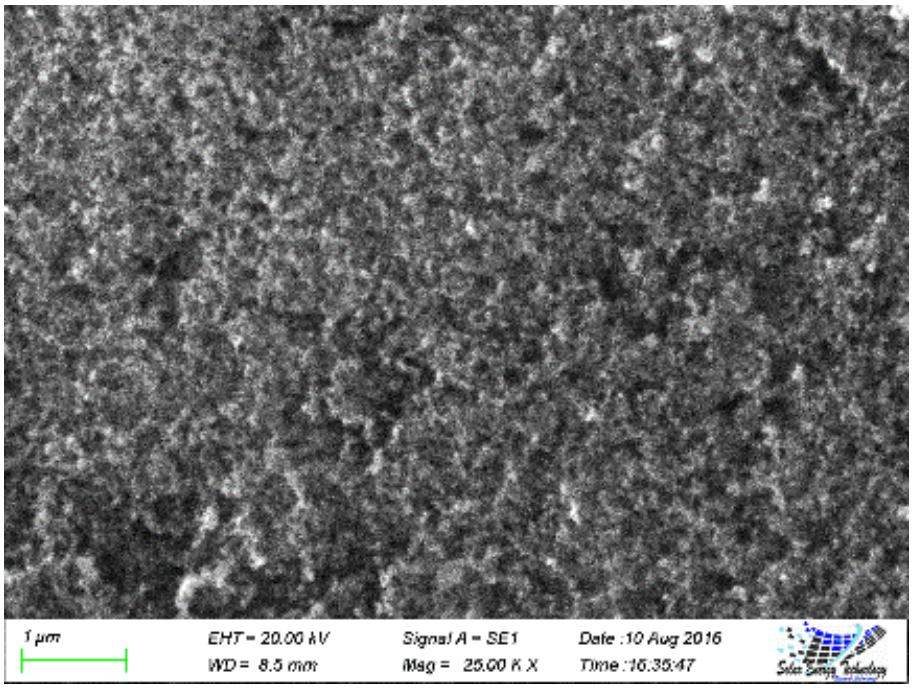

Figure 31 SEM image showing pores in TiO_2/dye coating

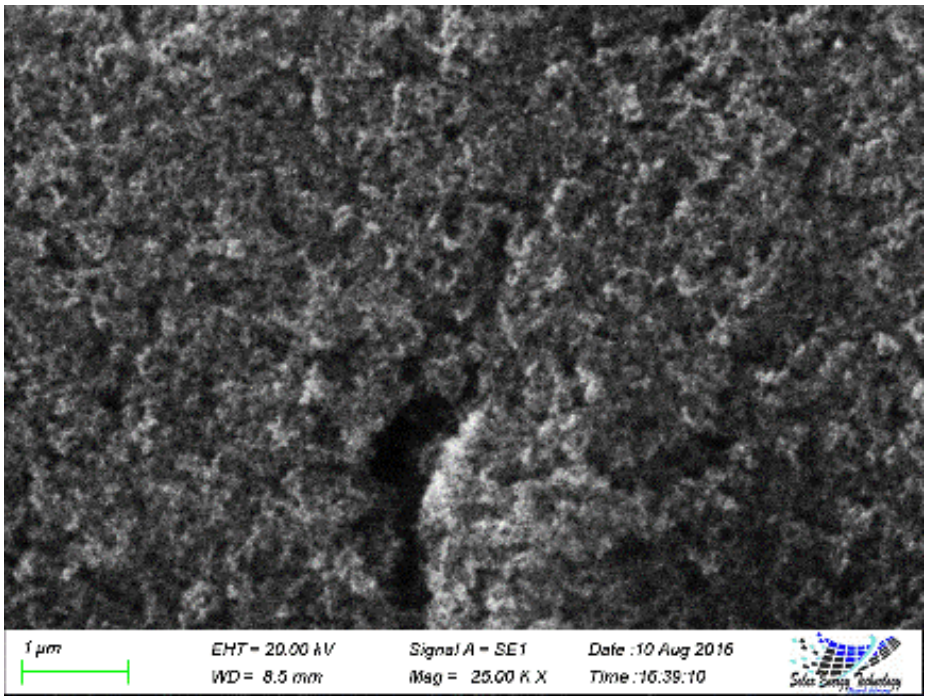

Figure 32 SEM image showing pores in TiO_2 coating

The application of dye causes the porosity of the titania layer to clearly and more distinctly visible. Presence of the porosity is advantageous to the cell performance due to the reduced recombination of the cell.

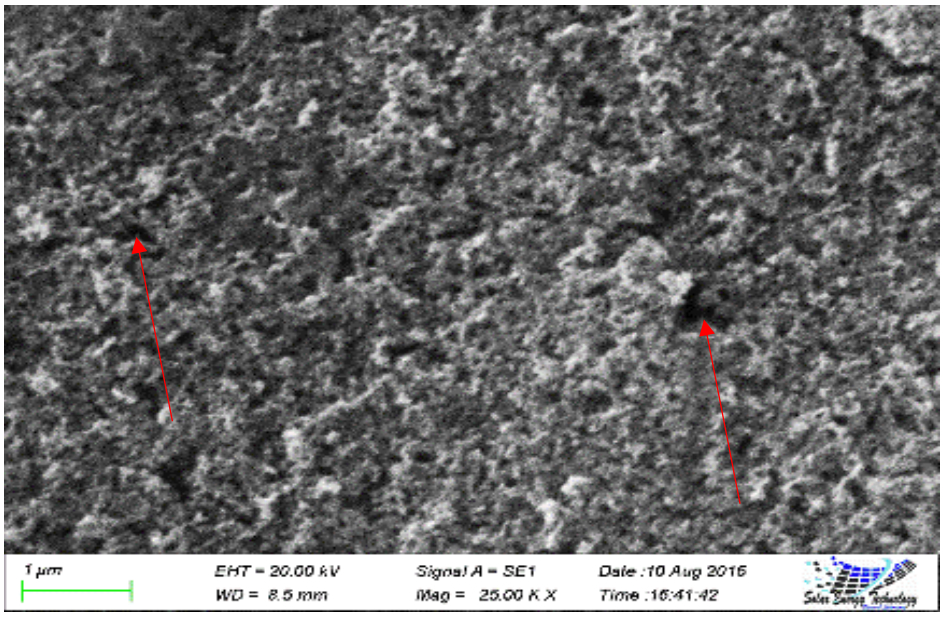

Figure 33 SEM image showing pores in post treated TiO_2 coating

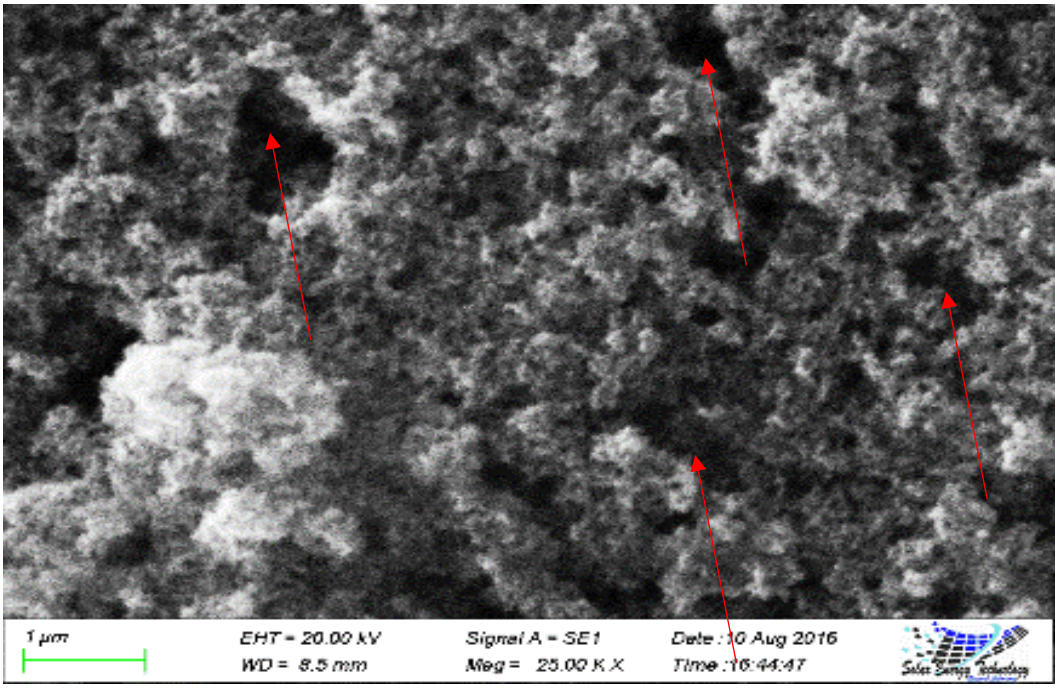

Figure 34 SEM image showing pores in post treated TiO_2/dye coating

The purpose of the blocking layer was to prevent charge recombination at the semiconductor/electrode interface, by preventing the electrolyte ions from reaching the electrode. Here in this research Chemical Bath Deposition techniques was applied for the deposition the thinnest possible blocking layer. The $TiCl_4$ treatment has increased the titania porosity clearly seen from the SEM images. However, for a titania film not optimized for porosity, the nano-porous film itself could effectively block the electrolyte. In that case, introduction of a blocking layer could just cause added series resistance reducing cell performance, which was probably the situation in these experiments.

5.1.3 UV-Visible Spectrophotometry

It is found that dyes extracted directly at room temperature have absorption peak at 430nm and 560nm (Fig. 35) corresponds to the absorption of around 3 a.u. Again, dyes extracted by ethanol have absorption peak which is not clearly visible in the figure (Fig. 36). The absorption spectrum for methanol and acetone was not performed to be included in this study. However, absorption peak would have been visibe had it not been so diluted. So, it can be assumed that extracted dyes having absorption peak of longer wavelengths will not be a good sensitizer. On the other hand, the energy associated with the absorption peak (430 nm) of ethanol, methanol, and acetone extracted dyes were near similar to the band gap energy of Degussa P25. So, mostly the energy associated with second absorption peaks are responsible for the transition of electron from the highest occupied molecular orbital (HOMO) to the lowest unoccupied molecular orbital (LUMO). Though ethanol, methanol, and acetone extracts showed almost same absorption peaks it was found that ethanol extract showed maximum cell efficiency which suggested that the pigment which responsible for the peak around 430 nm in ethanol extract have higher electron splitting ability compared to the pigments of ethanol and methanol extract.

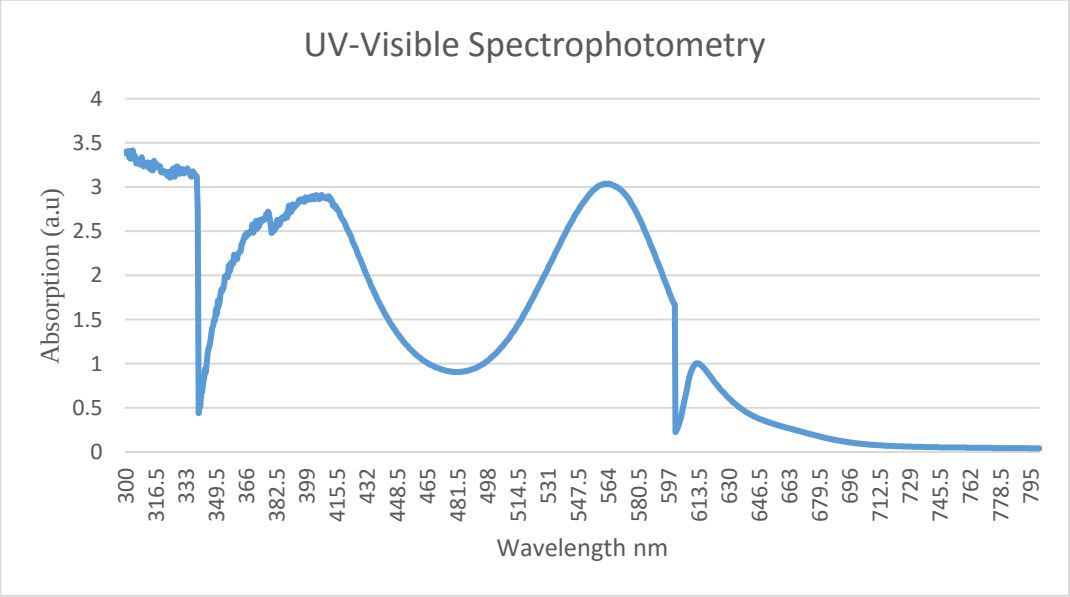

Figure 35 UV-visible spectrophotometry of raw dye

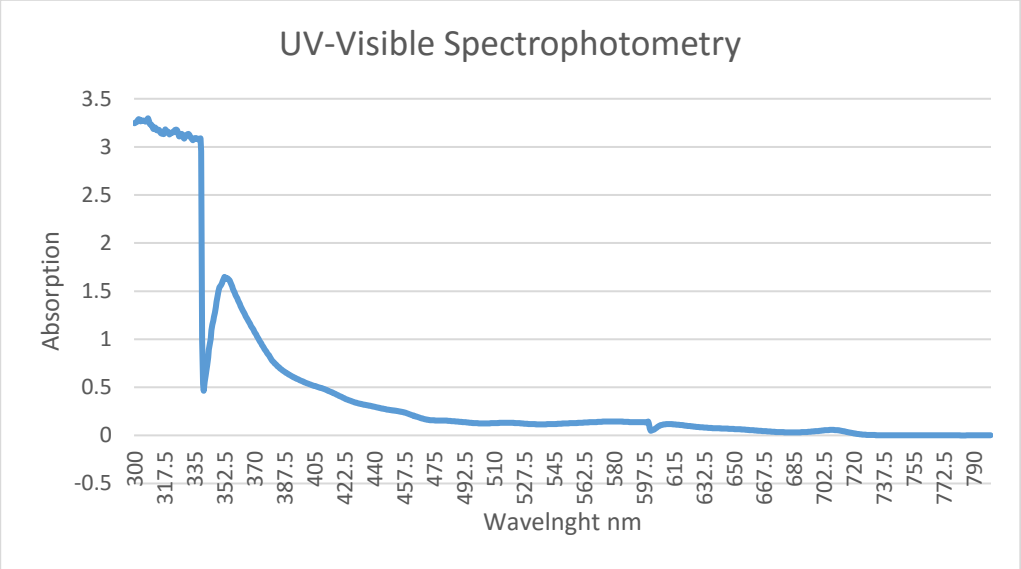

Figure 36 UV-visible spectrophotometry of dye in ethanol in diluted condition

5.1.4 FTIR spectroscopy

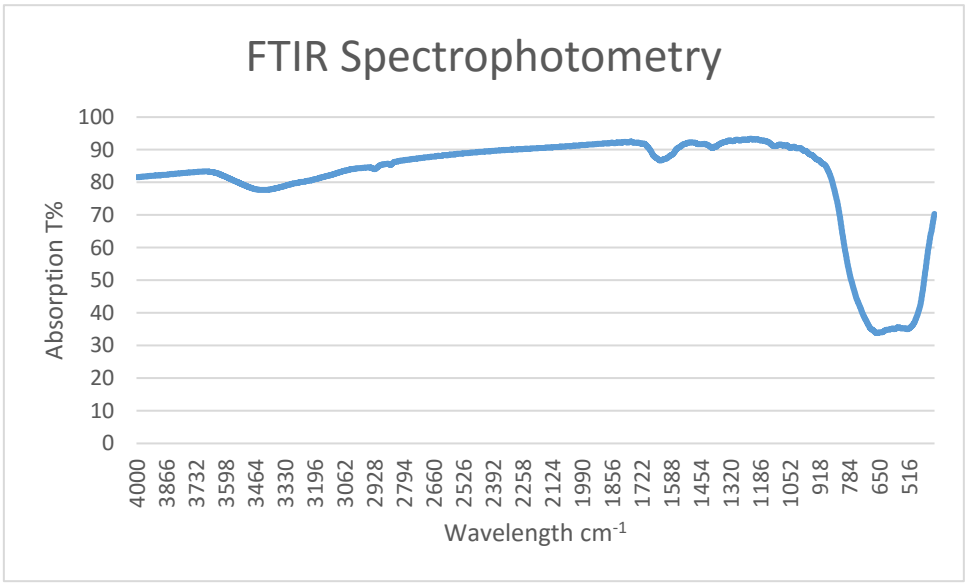

Figure 37 FTIR spectroscopy for TiO_2

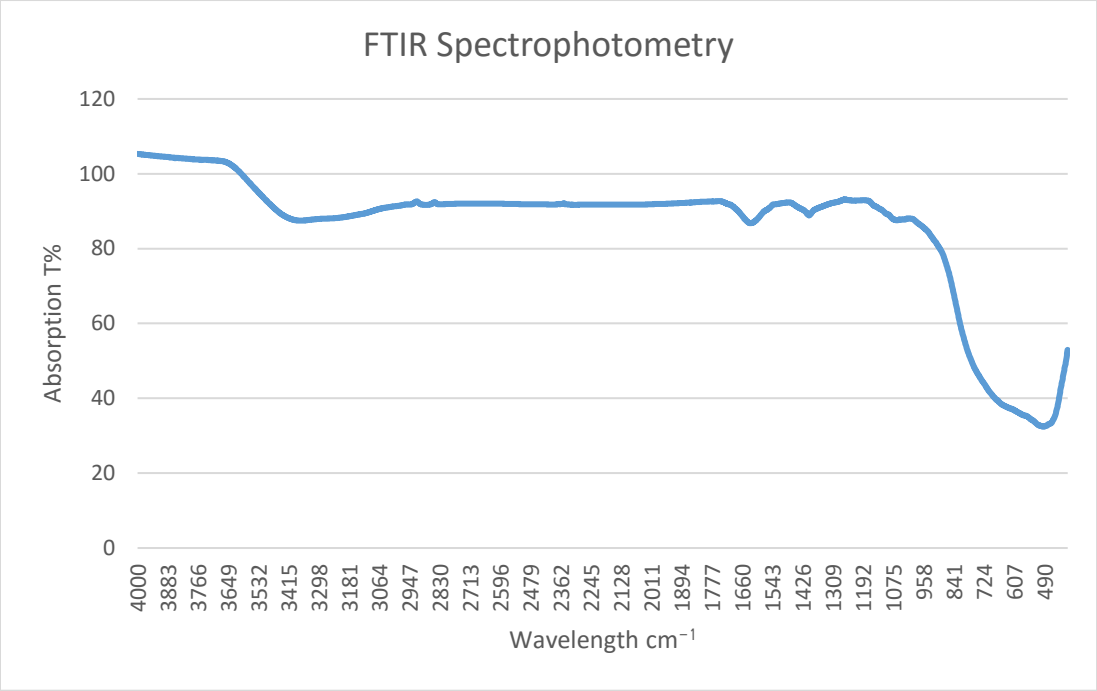

Figure 38 FTIR spectroscopy for TiO_2 and dye

The FTIR spectra of blackberry dye **(fig. 37)** shows a long and broad peak at 3395.74 cm-1 indicating the presence of hydrogen bonded O-H stretching of alcohols or phenols. Because, a sharp, strong and broad band is observed with in the region 3500~3700 cm-1 for free –OH or N-H stretching of primary alcohol or primary or secondary amines. A narrow peak observed at 1700.28 cm-1 may be attributed to C=O stretching of acid. Another long but weak band observed at 1645.31 cm-1may be due to the presence of C=C stretching unsaturated alkene or N-H bending vibration of primary amine. A slight peak 1013 cm^{-1} were assigned for C-O-C. A medium and narrow peak observed at 1369.48 cm-1 indicates the presence of C-H bending. A peak band observed at 1236.39 cm-1 may be due to the presence of C-O stretching vibration. Two bands observed at 1093.66 and 1020.36 cm-1 represent the presence of C-O stretching [26].

In the FTIR spectra of mixture of Degussa P25 and blackberry dye **(Fig. 38)** shows a long, broad and sharp peak at 3373.56 cm-1 which also indicates the presence of OH group of alcohol or phenol or N-H stretching of primary or secondary amine, as like as the spectra

of red amaranth dye (Fig. 38). Since the frequency of the peak slightly shifted in the lower frequency, it suggests that extra hydrogen bonding exists in -OH or N-H groups. The peaks 1636.63cm^{-1}which are almost similar to the spectra of blackberry dye (Fig. 38) assigned the presence of C-N stretching of amine and C=C stretching of unsaturated alkine or N-H bonding vibration of primary amine respectively. Another two insignificant but very weak peaks observed at 1401.31 and 1102.34 cm^{-1} may be due to the presence of C-C bending [26].

From the FTIR spectra of Degussa and blackberry dye mixture it has been shown that some peaks are absent in this spectra from the pure red amaranth dye, such as no peaks were observed at 1369.48, 1236.39, 1093.66, 1020.36 cm^{-1}. This occurred due to chemical modification or some component might be removed during washing the TiO_2 coated film soaked in black berry dye.

From the investigation of FTIR spectra of Degussa P25 and red amaranth dye (Fig. 38) it has been shown that it contains primary or secondary hydrogen bonded -OH groups or primary (-N-H) or secondary (–N-H) amino groups or both. When dyes are allowed to absorb photon from the sun light, this lone pair of electrons from –OH or amino (-N-H) groups are excited. These excited electrons transfer from valance band to conduction band and thus carried out electricity.

Chapter 6

6.1 CONCLUSION

The reserve of fossil fuel in the world is not unlimited. Renewable energy especially solar energy can play a vital role against this limited fossil fuel reservation. If the contribution of solar energy in our national energy consumption is to be high enough, we will ensure the energy supply for our next generation. So, to develop a credible solar cell technology is an epoch making step. With this view to produce a dye sensitized solar cell at a cost lower than conventional solar cell and maximum efficiency the main aim of my research was set.

According to this research performed it is clear that the use of the titanium tetrachloride solution as blocking agent has positive effect on the titania layer increasing current by around 500mV. As a result there is also improvements observed in the fill-factor and efficiency. The use of several different solvent to observe the effect has also shown that the anthocyanin group is most effective in presence of ethanol. The effect of pre-treatment by the titanium tetrachloride solution was also tried in this research. However, the obtained output was poor. Upon analysis it was found the use of ITO glass has an effect as a result hampering the result. ITO is acid sensitive. This has resulted in etching of the free area of the ITO glass when $TiCl_4$ treatment was done. As a result the data obtained was incorrectly interpreted affected. Upon further study it was found that Fluorine doped Tin Oxide (FTO) is acid insensitive.

To conclude this research, we believe that it has opened new scopes with change in dye extraction processes and of electrolyte may be applied to improve the photo-voltage and the reduction of resistance of the cell there by attempting for an improvement of efficiency can be considered in the next research.

6.2 FUTURE SCOPES

Due to limitation of available technologies and resources this study could not extend its boundaries. However, it leaves new horizon to be explored with new dyes and their effect on adsorption or soaking time. Furthermore the $TiCl_4$ treatment has not been optimized and could be performed. Application of the treatment both before and after (pre and post treatments together) on titanim dioxide coating is definitely another option. Most importantly use of FTO glasses during this treatments certainly has new scopes.

In a nut shell, this research work has a lot more potential regions for further study in future in the research and development sector.

Appendix I

Table 1 Voltage and Current data of a fabricated cell using raw blackberry dye

No.	V(mV)	I(mA)	P = (V*I)	P_{max}	I_m	V_m
I_{sc}	0	0.6	0	87.36	0	0
1	156	0.56	87.36	88.705	0	0
2	157	0.565	88.705	90.312	0	0
3	159	0.568	90.312	108.035	0	0
4	205	0.527	108.035	120.575	0	0
5	265	0.455	120.575	120.575	0.455	265
6	296	0.407	120.472	120.575	0	0
7	319	0.362	115.478	120.575	0	0
8	328	0.317	103.976	120.575	0	0
9	362	0.243	87.966	120.575	0	0
10	371	0.212	78.652	120.575	0	0
11	378	0.188	71.064	120.575	0	0
12	381	0.172	65.532	120.575	0	0
13	385	0.159	61.215	120.575	0	0
14	389	0.144	56.016	120.575	0	0
15	392	0.129	50.568	120.575	0	0
16	395	0.118	46.61	120.575	0	0
17	393	0.103	40.479	120.575	0	0
18	400	0.093	37.2	120.575	0	0
19	401	0.088	35.288	120.575	0	0
20	402	0.08	32.16	120.575	0	0
21	404	0.072	29.088	120.575	0	0
22	406	0.064	25.984	120.575	0	0
23	407	0.059	24.013	120.575	0	0
24	408	0.054	22.032	120.575	0	0
25	408	0.05	20.4	120.575	0	0
26	409	0.048	19.632	120.575	0	0
27	409	0.044	17.996	120.575	0	0
28	410	0.041	16.81	120.575	0	0
29	410	0.04	16.4	120.575	0	0
V_{oc}	440	0	0	120.575	0	0

Input Power	1000W
L (cm)	1.7
W (cm)	2.2
Area	3.74
$J_m=I_m/A$	0.12166
$J_{sc}=I_{sc}/A$	0.16043
Fill factor (FF)	0.4567235
Efficiency (η)	0.03224

6.2.1.2 Ethanol

Table 2 Voltage and Current data of a fabricated cell using ethanol soaked blackberry dye

No.	V(mV)	I(mA)	P = (V*I)	P_{max}	I_m	V_m
I_{sc}	0	0.943	0	190.34	0	0
1	307	0.62	190.34	190.34	0.62	307
2	318	0.564	179.352	190.34	0	0
3	378	0.386	145.908	190.34	0	0
4	395	0.333	131.535	190.34	0	0
5	418	0.146	61.028	190.34	0	0
6	435	0.149	64.815	190.34	0	0
7	445	0.141	62.745	190.34	0	0
8	451	0.118	53.218	190.34	0	0
9	455	0.102	46.41	190.34	0	0
10	458	0.096	43.968	190.34	0	0
11	461	0.085	39.185	190.34	0	0
12	465	0.073	33.945	190.34	0	0
13	467	0.065	30.355	190.34	0	0
14	469	0.058	27.202	190.34	0	0
15	471	0.055	25.905	190.34	0	0
16	472	0.052	24.544	190.34	0	0
17	473	0.051	24.123	190.34	0	0
18	474	0.05	23.7	190.34	0	0
19	475	0.048	22.8	190.34	0	0
20	478	0.046	21.988	190.34	0	0
V_{oc}	497	0	0	190.34	0	0

Input Power	1000W
L (cm)	1.7
W (cm)	2.2
Area	3.74
$J_m=I_m/A$	0.16578
$J_{sc}=I_{sc}/A$	0.25214
Fill factor (FF)	0.406127
Efficiency (**η**)	0.050889

6.2.1.3 Acetone

Table 3 Voltage and Current data of a fabricated cell using acetone soaked blackberry dye

No.	V(mV)	I(mA)	P = (V*I)	P_{max}	I_m	V_m
I_{sc}	0	0.7	0	53.24	0	0
1	88	0.605	53.24	54.873	0	0
2	91	0.603	54.873	95.445	0	0
3	189	0.505	95.445	127.35	0	0
4	283	0.45	127.35	127.35	0.45	283
5	305	0.363	110.715	127.35	0	0
6	311	0.35	108.85	127.35	0	0
7	330	0.349	115.17	127.35	0	0
8	365	0.248	90.52	127.35	0	0
9	380	0.23	87.4	127.35	0	0
10	398	0.182	72.436	127.35	0	0
11	407	0.17	69.19	127.35	0	0
12	412	0.148	60.976	127.35	0	0
13	413	0.133	54.929	127.35	0	0
14	417	0.122	50.874	127.35	0	0
15	420	0.121	50.82	127.35	0	0
16	423	0.108	45.684	127.35	0	0
17	426	0.101	43.026	127.35	0	0
18	432	0.089	38.448	127.35	0	0
19	433	0.084	36.372	127.35	0	0
20	436	0.08	34.88	127.35	0	0
21	437	0.1	43.7	127.35	0	0
22	438	0.072	31.536	127.35	0	0
23	439	0.066	28.974	127.35	0	0
24	440	0.062	27.28	127.35	0	0
25	441	0.059	26.019	127.35	0	0
26	443	0.05	22.15	127.35	0	0
27	444	0.048	21.312	127.35	0	0
28	445	0.047	20.915	127.35	0	0
29	450	0.044	19.8	127.35	0	0
V_{oc}	550	0	0	127.35	0	0

Input Power	1000W
L (cm)	1.7
W (cm)	2.5
Area	4.25
$J_m=I_m/A$	0.10588
$J_{sc}=I_{sc}/A$	0.01647
Fill factor (FF)	3.3078
Efficiency (**η**)	0.02996

6.2.1.4 Post treatment 70degrees

Table 4 Voltage and Current data of a post treated (at 70 degrees) fabricated cell

No.	V(mV)	I(mA)	P = (V*I)	P_{max}	I_m	V_m
I_{sc}	0	1.507	0	385.575	0	0
1	291	1.325	385.575	474.354	0	0
2	342	1.387	474.354	474.354	1.387	342
3	398	0.699	278.202	474.354	0	0
4	400	0.701	280.4	474.354	0	0
5	420	0.502	210.84	474.354	0	0
6	434	0.332	144.088	474.354	0	0
7	441	0.238	104.958	474.354	0	0
8	444	0.122	54.168	474.354	0	0
9	448	0.126	56.448	474.354	0	0
10	449	0.103	46.247	474.354	0	0
11	448	0.087	38.976	474.354	0	0
12	448	0.079	35.392	474.354	0	0
13	447	0.07	31.29	474.354	0	0
14	447	0.059	26.373	474.354	0	0
15	446	0.05	22.3	474.354	0	0
16	445	0.044	19.58	474.354	0	0
17	445	0.043	19.135	474.354	0	0
V_{oc}	453	0	0	474.354	0	0

Input Power	1000W
L (cm)	2.2
W (cm)	2.5
Area	2.5
$J_m=I_m/A$	0.25218
$J_{sc}=I_{sc}/A$	0.274
Fill factor (FF)	0.694850
Efficiency (**η**)	0.08625

6.2.1.5 Post treatment 12 hours

Table 5 Voltage and Current data of a post treated (for 12 hours) fabricated cell

No.	V(mV)	I(mA)	P = (V*I)	P_{max}	I_m	V_m
I_{sc}	0	0.976	0	4.947	0	0
1	51	0.097	4.947	4.947	0	0
2	52	0.043	2.236	5.459	0	0
3	53	0.103	5.459	5.459	0	0
4	53	0.099	5.247	5.885	0	0
5	55	0.107	5.885	8.624	0	0
6	56	0.154	8.624	8.624	0	0
7	56	0.109	6.104	8.624	0	0
8	57	0.124	7.068	10.208	0	0
9	58	0.176	10.208	11.092	0	0
10	59	0.188	11.092	11.34	0	0
11	60	0.189	11.34	11.34	0	0
12	60	0.17	10.2	14.72	0	0
13	64	0.23	14.72	19.338	0	0
14	66	0.293	19.338	21.692	0	0
15	68	0.319	21.692	21.692	0.319	68
16	69	0.327	22.563	21.692	0	0
17	71	0.332	23.572	21.692	0	0
18	72	0.366	26.352	21.692	0	0
19	73	0.423	30.879	21.692	0	0
20	77	0.451	34.727	21.692	0	0
21	78	0.544	42.432	21.692	0	0
22	79	0.885	69.915	21.692	0	0
23	79	0.519	41.001	21.692	0	0
24	86	0.997	85.742	21.692	0	0
25	95	1.319	125.305	21.692	0	0
26	119	1.326	157.794	21.692	0	0
27	136	1.331	181.016	21.692	0	0
V_{oc}	480	0	0	21.692	0	0

Input Power	1000W
L (cm)	1.7
W (cm)	2.5
Area	4.25
$J_m=I_m/A$	0.07506
$J_{sc}=I_{sc}/A$	0.22965
Fill factor (FF)	0.0463
Efficiency (**η**)	0.0051

REFERENCES

[1] R. H. a. A. Mohammadi, "Improving optical absorptivity of natural dyes for fabrication of efficient dye-sensitized solar cells," *Journal of Theoretical and Applied Physics,* vol. 57, no. 7, 2013.

[2] Y. C. C. J.-H. R. J. H. K. ,. N. K. P. ,. D. K. L. &. J. H. K. Hyo Jeong Jo, "Synthesis and Characterization of Organic Photosensitizers Containing Multi-Acceptors for the Application of Dye-sensitized Solar Cells," *Molecular Crystals and Liquid Crystals,* vol. 532, pp. 471-480, 2010.

[3] T. R. H. &. L. Cindrella, "Molecular Orbital Evaluation of Charge Flow Dynamics in Natural Pigments Based Photosensitizers," *Journal of Molecular Modeling* , vol. 16, p. 523–533, 2010.

[4] M. G. B. O'Regan, "A low-cost, high efficiency solar cell based on dye-sensitized colloidal TiO2 films," *Nature,* pp. 737-740, 1991.

[5] M. Grätzel, "Photoelectrochemical cells," *Nature,* vol. 414, no. 6861, pp. 338-344, 2001. .

[6] M. G. A. Hagfeldt, "Molecular Photovoltaics," *Acc. Chem.,* vol. 33, p. 269, 2001.

[7] C. B. a. R. A. G. Smestad, "Testing of dye sensitized $Ti0_2$ solar cells I: Experimental photocurrent output and conversion efficiencies," *Solar Energy Materials and Solar Cells,* vol. 32, p. 259, 1994.

[8] R. &. M. A. J. Hemmatzadeh, "Improving optical absorptivity of natural dyes for fabrication of efficient dye-sensitized solar cells," *Journal of Theoretical and Applied Physics,* vol. 7, p. 57, 2013.

[9] Q. W. L. &. H. S. S. E. Lin, "Effects of different treatment of TiO2 electrodes on photovoltaic characteristics of dye-sensitized solar cells," *Surface Engineering and Applied Electrochemistry,* vol. 51, no. 4, p. 394–400, 2015.

[10] J.-G. M. R. V. M. Hamadanian, "Uses of New Natural Dye Photosensitizers in Fabrication of High Potential Dye Sensitized Solar Cell (DSSCs)," *Materials Science in Semiconductor Processing,* vol. 27, p. 733–739, 2014.

[11] J.-H. Y. A. S. G. D. M. M. G. M. K. N. Giuseppe Calogero, "Anthocyanins and Betalains as Light-Harvesting igments for DYe-Sensitized Solar Cell," *Solar Energy,* vol. 86, p. 156301575, 2012.

[12] E. R.-R. F. C.-R. J. A. R.-d.-L. M. V. Eddie Nahum Armendariz-Mireles, "Photocurrent Generation by Dye-Sensitized Solar Cell Using Natural Pigments," *Biotechnology and Applied Biochemistry,* 2015.

[13] M. H. G. D. S. C. a. S. P. K. Hailey E. Cramer, "Green Nanochemistry Approach to Titanium Dioxide NAnoparticle Dye-Sensitized Solar Cell," 2012.

[14] H. P. U. a. J. D. Stephen Lourens Tanihaha, "Fabrication and Characterization of Dye-sensitized Solar Cell using Blackberry Dye and Titanium Dioxide Nanocrystal," in *Second International Conference on Advances in Computing, Control, and Telecommunication Technologies,* 2010.

[15] M. C. L. J. V. J. M. C. A. F. Z. R. CANALS, "Influence of Ethanol Concentration on the Extraction of Color and Phenolic Compounds from the Skin and Seeds of Tempranillo Grapes at Different Stages of Ripening," *Journal of Agricultural and Food Chemistry,* vol. 53, pp. 4019-4025, 2015.

[16] R. R. G. S. T. M. B. A. D. C. A. R. Luigi Vesce, "Optimization of nanostructured titania photoanodes for dye-sensitized solar cells: Study and Experimentation of TiCl4 Treatment," *Journal of Non-Crystalline Solids,* vol. 356, p. 1958–1961, 2010.

[17] A. S. a. H. N. Miankushki, "Influence of TiCl4 Treatment on Structure and Performance of Dye-Sensitized Solar Cells," *Japanese Journal of Applied Physics,* vol. 52, pp. 075002-1-075002-6, 2013.

[18] B. C. O. R. R. H. H. J. P. S. N. J. B. J. J. T. S. J. M. K. a. J. A. M. v. R. P. M. Sommeling, "Influence of a TiCl4 Post-Treatment on Nanocrystalline TiO2 Films in Dye-Sensitized Solar Cells," *Journal of Physical Chemistry,* vol. 110, pp. 19191-19197, 2006 .

[19] S. M. Z. ,. P. C. ,. R. C. ,. R. H.-B. ,. a. M. G. Peng Wang, "Enhance the Performance of Dye-Sensitized Solar Cells by Co-grafting Amphiphilic Sensitizer and Hexadecylmalonic Acid on TiO2 Nanocrystals," *Journal of Physical CHemistry B,* vol. 107, no. 51, pp. 14336-14341, 2003.

[20] D. A. P. N. K. K. G. M. Bonhôte P1, "Hydrophobic, Highly Conductive Ambient-Temperature Molten Salts," *Inorganic Chemistry,* vol. 5, no. 35, pp. 1168-1178, 1996.

[21] S. Z. R. H.-B. M. J. P. L. ,. N. V. ,. V. S. ,. C.-H. F. ,. a. M. G. Md. K. Nazeeruddin, "Acid−Base Equilibria of (2,2‘-Bipyridyl-4,4‘-dicarboxylic acid)ruthenium(II) Complexes and the Effect of Protonation on Charge-Transfer Sensitization of Nanocrystalline Titania," *Inorganic Chemistry,* vol. 26, no. 38, p. 6298–6305, 1999.

[22] D. A. F. F. S. S. A. V. G. L. P. I. S. T. B. G. M. Nazeeruddin MK1, "Combined experimental and DFT-TDDFT computational study of photoelectrochemical cell ruthenium sensitizers," *Journal of American Çhemical Society,* vol. 48, no. 127, pp. 16835-47, 2005.

[23] F. P. ,. S. F. ,. a. C. L. F. Brian A. Gregg, "Interfacial Recombination Processes in Dye-Sensitized Solar Cells and Methods To Passivate the Interfaces," *Journal of Physical Chemistry B,* vol. 7, no. 105, p. 1422–1429, 2001.

[24] E. A. S. N. G. P. J. v. d. L. a. A. J. F. Kai Zhu, "Determining the Locus for Photocarrier in Dye Sensitized Solar Cell," *APPLIED PHYSICS LETTERS,* vol. 80, pp. 685-687, 2002.

[25] P. L. A. Kosyachenko, "Investigation of Dyes for Dye-Sensitized," in *Solar Cells – Dye-Sensitized Devices* , Intech, 2011, pp. 19-46.